JOURNAL OF THE AERO/SPACE SCIENCES

VOLUME 26 SEPTEMBER, 1959 NUMBER 9

The Determination of Round-Trip Planetary Reconnaissance Trajectories

RICHARD H. BATTIN*

Massachusetts Institute of Technology

Summary

Some interesting geometrical and analytical properties of free fall trajectories are developed and subsequently exploited to provide a technique for determining interplanetary transfer orbits. After a general discussion, the determination of propulsion-free round trips to the planet Mars is considered. As a preliminary step, the reconnaissance problem is analyzed for a simple two-dimensional model of the solar system, assuming circular planetary orbits.

Finally, a method is described for determining round-trip, nonstop reconnaissance trajectories in a three-dimensional model with elliptical planetary orbits. The results from the simplified approach are compared with those obtained from the true model. It is found that several important features of the trajectory problem are basically three-dimensional in nature and that the simplified model is inadequate for their description.

(1) Geometrical and Analytical Properties of Trajectories

(1.1) *General Conic Trajectories*

WHEN A BODY is in motion under the action of an attractive central force that varies as the inverse square of the distance, the path described will be a conic whose focus is at the center of attraction. The particular conic (ellipse, hyperbola, or parabola) is determined solely by the velocity and the distance from the center of force. In many problems of interplanetary flight it is frequently convenient to analyze the flight of a space ship by considering its motion to be influenced by only one celestial body during any one period of time. Therefore, we shall begin our study of interplanetary trajectories by considering the purely geometrical problem of determining the various conic paths that connect two fixed points and that have a focus coinciding with a fixed center of force.

Presented at the Space Flight Mechanics Session, Twenty-Seventh Annual Meeting, IAS, New York, January 26–29, 1959.

* Assistant Director, Instrumentation Laboratory, Department of Aeronautics and Astronautics.

There are many equivalent definitions of conics; however, we shall find the following ones most convenient for our purposes:

Ellipse: The locus of points the sum of whose distances from two fixed points (foci) is constant.

Hyperbola: The locus of points the difference of whose distances from two fixed points (foci) is constant.

Parabola: The locus of points equally distant from a fixed point (focus) and a fixed straight line (directrix).

The familiar elements of these conics are shown in Figs. 1-1, 1-2, and 1-3 and will serve to orient the reader during the remainder of the discussion.

Consider now two fixed points P and Q and a center of force fixed at a point F. For parabolic paths these three points are sufficient to determine the two parabolas connecting P and Q with a focus at F. However, for elliptic and hyperbolic paths, further specifications are required to determine a unique trajectory. Let us examine first the characteristics of the family of elliptical paths.

(1.2) *Elliptical Trajectories*

Consider the three points F, P, and Q in Fig. 1-4 and let it be required to find an ellipse with a focus at F that connects the two points P and Q. If the location of the second focus F^* (sometimes called the vacant focus) is fixed, the problem is solved and the path is determined. Since the point F^* cannot be placed arbitrarily, it will be of interest to find the locus of the foci of all ellipses that satisfy the conditions of the problem.

To this end, let us designate the line segments in Fig. 1-4 as follows:

$$FP = r_1, \quad FQ = r_2, \quad PQ = c \qquad (1.2.1)$$

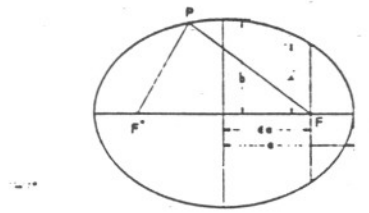

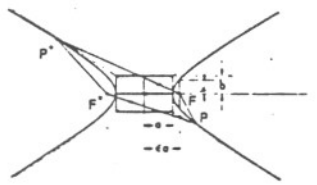

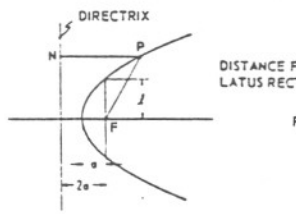

FIG. 1-1 (*Top*). Ellipse. FIG. 1-2 (*Center*). Hyperbola. FIG. 1-3 (*Bottom*). Parabola.

(In our discussion we shall assume $r_2 > r_1$; obvious changes in the results can be made if the reverse inequality holds. The case for which $r_1 = r_2$ is quite special and, indeed, almost trivial.) Since P and Q must both lie on the ellipse, the point F^* must be selected such that

$$PF^* + PF = QF^* + QF = 2a$$

or, equivalently,

$$PF^* = 2a - r_1, \quad QF^* = 2a - r_2$$

Thus, for an ellipse of major axis $2a$, the point F^* is determined as the point of intersection of two circles centered at P and Q with respective radii $2a - r_1$ and $2a - r_2$. A number of such circles have been constructed in Fig. 1-4 for different values of the major axis $2a$.

We may make at once several interesting observations:

(a) If the selected value of $2a$ is too small, the circles will not intersect. Thus, there is a smallest value, $2a_m$, below which no elliptical path is possible. When $a = a_m$, the two circles are tangent and the point of tangency F_m^* lies on the line PQ. Thus, a_m may be determined from

$$(2a_m - r_2) + (2a_m - r_1) = c$$

to give a value

$$2a_m = (r_1 + r_2 + c)/2 \qquad (1.2.2)$$

which is just one-half of the perimeter of the triangle FPQ. For later convenience, we introduce the notation

$$2s = r_1 + r_2 + c \qquad (1.2.3)$$

so that

$$2a_m = s$$

The point F_m^* divides the line PQ in such a way that

$$PF_m^* = s - r_1, \quad QF_m^* = s - r_2$$

(b) When $a > a_m$, the pair of circles intersect in two points F^* and $\bar{F}^*$. Thus, there are, in general, two different elliptical paths connecting P and Q having the same length major axis but with vacant foci equidistant from and falling on opposite sides of the line PQ. For any value of $2a$, the focus $\bar{F}^*$ is a greater distance from F than the corresponding conjugate focus F^*. Therefore, the ellipse with focus at $\bar{F}^*$ has a larger eccentricity and a smaller latus rectum than the ellipse with the same length major axis and focus at F^*.

As a point of interest, the values of a_1 and a_2 used in the construction of Fig. 1-4 are

$$2a_1 = 2a_m + r_1/2, \quad 2a_2 = 2a_m + r_1$$

(c) Each vacant focus is so located that the distances from P and Q have a constant difference $r_2 - r_1$. Thus, the locus of these foci is a hyperbola; P and Q are the foci of the hyperbola; $r_2 - r_1$ is the length of its major axis; and $c/(r_2 - r_1)$ is the eccentricity. The asymptotes of the hyperbola have slopes given by

$$\text{Slopes of the asymptotes} = \pm [2/(r_2 - r_1)] \sqrt{(s - r_1)(s - r_2)} = \pm [2\sqrt{r_1 r_2}/(r_2 - r_1)] \sin(\theta/2) \qquad (1.2.4)$$

The second form of Eq. (1.2.4) shows explicitly how the hyperbolic locus of F^* varies with the angle between FP and FQ.

Minimum-Energy Ellipse

The point F_m^* defines the so-called "minimum-energy" elliptical path from P to Q. The kinetic energy of a body, moving in free fall along an elliptical arc, is proportional to $[(1/r) - (1/2a)]$, where r is the distance from the center of force. Thus, the kinetic energy at any point is a minimum when the major axis of the path has the minimum value of $2a_m$. We may determine the semi-latus rectum l_m and the eccentricity ϵ_m of the minimum energy path in the following manner:

Since $\epsilon = \frac{\quad}{\quad}$ $\qquad FF_m^* = 2\epsilon_m a_m$

we have, from Fig. 1-4,

$$(2\epsilon_m a_m)^2 = [(s - r_2) \sin \angle PQF]^2 + [r_2 - (s - r_2) \cos \angle PQF]^2$$

Using the trigonometric identity

$$\cos \angle PQF = [2s(s - r_1)/r_2 c] - 1$$

we have

$$(2\epsilon_m a_m)^2 = s^2 - 4s(s - r_1)(s - r_2)/c$$

But, for an ellipse, in general,

$$(2\epsilon a)^2 = 4a(a - l)$$

so that $(2\epsilon_m a_m)^2 = s^2 - 2sl_m$

Hence,

$$l_m = 2(s - r_1)(s - r_2)/c = (r_1 r_2/c)(1 - \cos\theta) \quad (1.2.5)$$

The eccentricity ϵ_m may then be found from

$$l_m = (s/2)(1 - \epsilon_m^2)$$

Osculating Ellipse

The point Q coincides with the point of aphelion for the ellipse whose focus F_1^* is determined as the intersection of the hyperbolic locus and the line QF. All elliptical paths from P to Q with foci to the right of the line QF reach aphelion before arriving at Q, while those with foci on the left reach aphelion after passing through Q. Since the path is tangent at Q to a circle of radius r_2 and centered at F, we shall use the term "osculating ellipse" when referring to this trajectory. We may again employ simple geometrical arguments to determine the major axis $2a_0$, eccentricity ϵ_0, and latus rectum l_0.

Referring to Fig. 1-4, we have, from the definition of an ellipse,

$$QF_0^* + QF = PF + PF_0^* = 2a_0$$

However, since Q, F, F_0^* are colinear, then

$$QF_0^* = r_2 - 2\epsilon_0 a_0 = 2a_0 - r_2$$

Hence, $$PF_0^* = 2r_2 - 2\epsilon_0 a_0 - r_1$$

Considering now the triangle FPF_0^*, we use a fundamental trigonometric identity to obtain

$$\frac{r_2[r_2 - (2r_2 - 2\epsilon_0 a_0 - r_1)]}{r_1(2\epsilon_0 a_0)} = \frac{1 + \cos\theta}{2}$$

which may be solved for $2\epsilon_0 a_0$ to yield

$$2\epsilon_0 a_0 = 2r_2(r_2 - r_1)/[2r_2 - r_1(1 + \cos\theta)]$$

But $$2a_0 = 2r_2 - 2\epsilon_0 a_0$$

so that

$$a_0 = r_2/\{1 + [(r_2 - r_1)/(r_2 - r_1\cos\theta)]\} \quad (1.2.6)$$

The corresponding value of the semi-latus rectum is readily found to be

$$l_0 = [r_1 r_2/(r_2 - r_1\cos\theta)](1 - \cos\theta) \quad (1.2.7)$$

Finally, by comparing Eqs. (1.2.5) and (1.2.7), we note the following interesting relation:

$$l_m = l_0 \cos \angle PQF \quad (1.2.8)$$

Symmetrical Ellipse

To complete our discussion of elliptical trajectories, let us consider the ellipse whose focus F_s^* is determined as the intersection of the hyperbolic locus and the line through F that is parallel to PQ. This path is of some interest because of its symmetry—i.e., the point P bears the same relationship to perihelion as the point Q does to aphelion. The elements of this ellipse, $2a_s$, ϵ_s, and l_s, are readily obtained since the polygon PQF_s^*F is an isosceles trapezoid.

We find $$2a_s = r_1 + r_2 \quad (1.2.9)$$

and

$$l_s = [r_1 r_2(r_1 + r_2)/c^2](1 - \cos\theta) = [(r_1 + r_2)/c]l_m \quad (1.2.10)$$

(1.3) *Hyperbolic Trajectories*

Consider again the three points F, P, and Q shown now in Fig. 1-5 and let it be required to find a hyperbola with focus at F that connects the two points P and Q. Again the problem is solved if the location of the second focus F^* is determined. However, since the point F is an attractive focus, we are interested only in the branch of the hyperbolic path that is concave with respect to F.

The points P and Q must both lie on the concave branch of the hyperbola, so that the point F^* must be selected such that

$$PF^* - PF = QF^* - QF = 2a$$

Thus, for a hyperbola whose major axis is $2a$, the point F^* is determined as the point of intersection of two circles centered at P and Q, with respective radii $2a + r_1$ and $2a + r_2$. Three such pairs of circles have

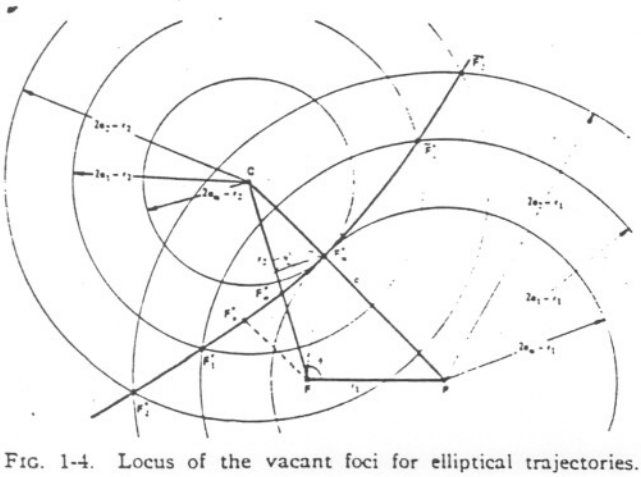

FIG. 1-4. Locus of the vacant foci for elliptical trajectories.

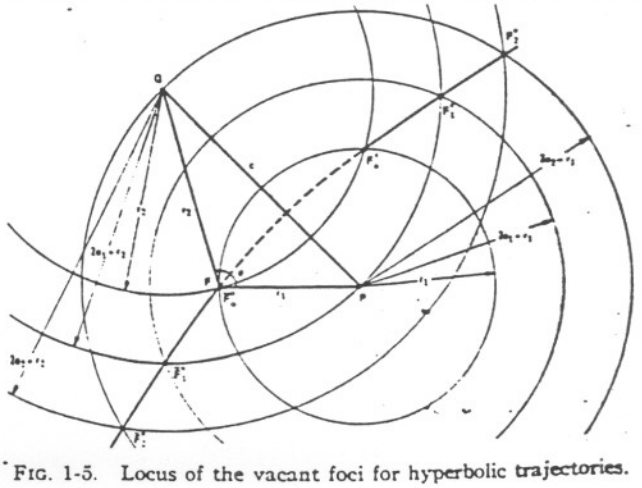

FIG. 1-5. Locus of the vacant foci for hyperbolic trajectories.

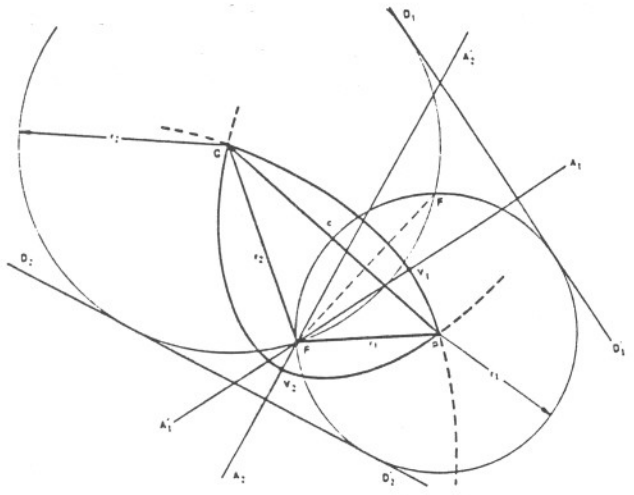

FIG. 1-6. Parabolic trajectories.

been constructed in Fig. 1-5 for values of $a = 0$, a_1, and a_2, where a_1 and a_2 where chosen as

$$2a_1 = r_1/2, \quad 2a_2 = r_1$$

We make the following interesting observations:

(a) All points of intersection of the circle pairs fall outside of the circle centered at P and of radius r_1. One may readily verify that, for hyperbolic paths from P to Q that are convex with respect to the focus F, the vacant foci F^* all lie within this circle.

(b) The pair of circles intersect in two points F^* and $\bar{F}^*$, so that there are two different hyperbolic paths connecting P and Q having the same length major axis and with vacant foci equidistant from and falling on opposite sides of the line PQ. For any value of $2a$, the hyperbola with focus at F^* has a larger eccentricity and a larger latus rectum than the corresponding hyperbola with focus at $\bar{F}^*$.

(c) Each vacant focus is so located that the difference of its distances from Q and P is $r_2 - r_1$. Thus, the locus of these foci is the conjugate branch of the hyperbolic locus of the foci for the elliptical paths considered previously.

The foci F_0^* and $\bar{F}_0^*$, corresponding to a zero-length major axis, are extreme cases in that infinite velocities are required to describe the associated paths. The path with vacant focus at F_0^* is the straight line from P to Q; i.e., the hyperbola for which $a = 0$ and $\epsilon = \infty$. Corresponding to the focus, $\bar{F}_0^*$, the path is composed of the two straight-line segments from P to F and from F to Q and is the hyperbola for which $a = 0$ and $\epsilon = \sec(\theta/2)$.

(1.4) *Parabolic Trajectories*

There are two parabolic paths with focus at F that connect the two points P and Q. To determine the axes of these parabolas, we shall first locate their directrices. Referring to Fig. 1-6 and recalling the definition of a parabola, the directrices D_1D_1' and D_2D_2' are obtained as the two common tangents of the two circles centered at P and Q with respective radii r_1 and r_2. The axes A_1A_1' and A_2A_2' of the two parabolas are the normals to the corresponding directrices through the focus F. The vertices V_1 and V_2 are the midpoints of that portion of the axes included between the focus F and the directrices. By elementary geometry one can show that the axes A_1A_1' and A_2A_2' are parallel to the asymptotes of the hyperbolic locus of the vacant foci of the elliptical and hyperbolic paths considered previously. Thus, Eq. (1.2.4) gives the slopes of these axes with respect to the line PQ.

Again, it is an elementary exercise in geometry to determine for each parabola the semi-latus rectum or, equivalently, the distance from focus to directrix. One obtains

$$l_1 = 2FV_1 = [\tfrac{1}{4}(s - r_1)(s - r_2)/c^2] \times [\sqrt{s/2} + \sqrt{(s - c)/2}]^2 \quad (1.4.1)$$

$$l_2 = 2FV_2 = [\tfrac{1}{4}(s - r_1)(s - r_2)/c^2] \times [\sqrt{s/2} - \sqrt{(s - c)/2}]^2 \quad (1.4.2)$$

(1.5) *Latus Rectum and Eccentricity*

Although we have found it possible to obtain the latus rectum and eccentricity of several special conic paths by employing geometrical arguments, it would be impractical to use similar techniques for the general case. Instead, let us tackle the problem of obtaining an analytic functional relationship between the latus rectum and major axis of the conic by using the polar-coordinate equation

$$r = l/(1 + \epsilon \cos \phi) \quad (1.5.1)$$

where r and ϕ are polar coordinates of a point on the conic whose focus is at the origin. The conic is either an ellipse or a hyperbola, according to whether the eccentricity ϵ is less than or greater than one, respectively. The semi-latus rectum l is related to the eccentricity ϵ and the semi-major axis a by

$$l = a(1 - \epsilon^2) \quad \text{(ellipse)} \quad (1.5.2)$$

$$l = a(\epsilon^2 - 1) \quad \text{(hyperbola)} \quad (1.5.3)$$

Since the points P and Q of Fig. 1-7 both lie on the conic, then, from Eq. (1.5.1), we have

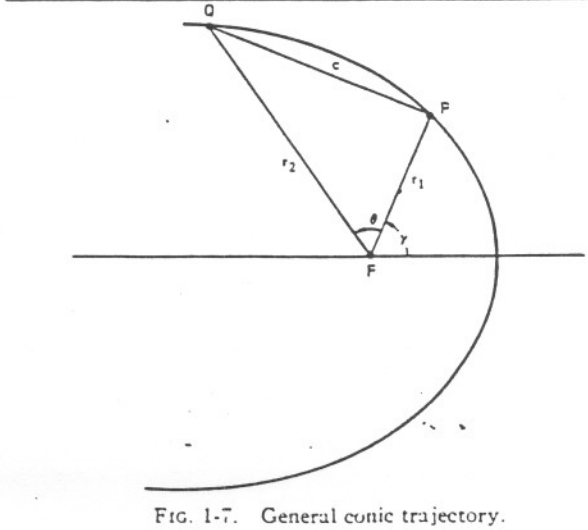

FIG. 1-7. General conic trajectory.

$$\epsilon \cos \gamma = (l/r_1) - 1, \quad \epsilon \cos (\gamma + \theta) = (l/r_2) - 1 \tag{1.5.4}$$

Consider the trigonometric identity

$$\cos^2 (\gamma + \theta) - 2 \cos (\gamma + \theta) \cos \gamma \cos \theta + \cos^2 \gamma - \sin^2 \theta = 0$$

and substitute from Eqs. (1.5.1)–(1.5.3) to obtain

$$ar_1^2(l - r_2)^2 - 2ar_1r_2(l - r_2)(l - r_1) \cos \theta + ar_2^2(l - r_1)^2 - (a \mp l)r_1^2r_2^2 \sin^2 \theta = 0$$

where the selection of upper or lower signs in the last term is made, respectively, according to whether the conic is an ellipse or a hyperbola. If we now collect terms in powers of l (note that the coefficient of l^2 is simply ac^2) and make further obvious simplifications, we find

$$ac^2l^2 - r_1r_2(1 - \cos \theta)[2a(r_1 + r_2) \mp r_1r_2(1 + \cos \theta)]l + ar_1^2r_2^2(1 - \cos \theta)^2 = 0 \tag{1.5.5}$$

Introducing the symbol s, which is defined by Eq. (1.2.3), permits the bracketed expression of Eq. (1.5.5) to be rewritten in the form

$$2a(r_1 + r_2) \mp r_1r_2(1 + \cos \theta) = 2a(2s - c) \mp 2s(s - c) = \mp 2s(s - c \mp 2a) - 2ac \tag{1.5.6}$$

In the remaining part of the derivation we shall consider separately the ellipse and the hyperbola.

For the elliptical case, it is convenient to introduce the notation

$$\sin(\alpha/2) = \sqrt{(r_1 + r_2 + c)/4a} = \sqrt{s/2a} \tag{1.5.7}$$

$$\sin (\beta/2) = \sqrt{(r_1 + r_2 - c)/4a} = \sqrt{(s - c)/2a} \tag{1.5.8}$$

so that we may write

$$s - c - 2a = -2a \cos^2 (\beta/2)$$
$$s = 2a \sin^2 (\alpha/2)$$
$$c = 2a [\sin^2 (\alpha/2) - \sin^2 (\beta/2)]$$

The right-hand side of Eq. (1.5.6) may then be written as

$$8a^2 \sin^2 (\alpha/2) \cos^2 (\beta/2) - 4a^2[\sin^2 (\alpha/2) - \sin^2 (\beta/2)] = 4a^2 \sin^2 (\alpha/2) \cos \beta + 4a^2 \sin^2 (\beta/2) = 2a^2\{\sin^2 [(\alpha + \beta)/2] + \sin^2 [(\alpha - \beta)/2]\}$$

Substituting this into Eq. (1.5.5) and further noting that

$$r_1r_2(1 - \cos \theta) = 2(s - r_1)(s - r_2)$$

gives

$$ac^2l^2 - 4a^2(s - r_1)(s - r_2)\{\sin^2 [(\alpha + \beta)/2] + \sin^2 [(\alpha - \beta)/2]\} l + 4a(s - r_1)^2(s - r_2)^2 = 0$$

Finally, multiplying through by c^2/a and using the identity

$$c = 2a \sin [(\alpha + \beta)/2] \sin [(\alpha - \beta)/2]$$

yields

$$c^2l^2 - 4a(s - r_1)(s - r_2)\{\sin^2 [(\alpha + \beta)/2] + \sin^2 [(\alpha - \beta)/2]\} c^2l + 16a^2(s - r_1)^2 (s - r_2)^2 \times \sin^2 [(\alpha + \beta)/2] \sin^2 [(\alpha - \beta)/2] = 0$$

from which the two roots

$$l = [4a(s - r_1)(s - r_2)/c^2] \times \sin^2 [(\alpha \pm \beta)/2] \quad \text{(ellipse)} \tag{1.5.9}$$

are obtained.

For the hyperbolic case, an analogous procedure is followed after introducing the notation

$$\sinh (\alpha/2) = \sqrt{(r_1 + r_2 + c)/4a} = \sqrt{s/2a} \tag{1.5.10}$$

$$\sinh (\beta/2) = \sqrt{(r_1 + r_2 - c)/4a} = \sqrt{(s - c)/2a} \tag{1.5.11}$$

We may then write

$$s - c + 2a = 2a \cosh^2 (\beta/2)$$
$$s = 2a \sinh^2 (\alpha/2)$$
$$c = 2a [\sinh^2 (\alpha/2) - \sinh^2 (\beta/2)]$$

and the right-hand side of Eq. (1.5.6) becomes

$$2a^2\{\sinh^2 [(\alpha + \beta)/2] + \sinh^2 [(\alpha - \beta)/2]\}$$

Substituting into Eq. (1.5.5), using the identity

$$c = 2a \sinh [(\alpha + \beta)/2] \sinh [(\alpha - \beta)/2]$$

and following the same steps as for the elliptical case, we obtain

$$l = [4a(s - r_1)(s - r_2)/c^2] \times \sinh^2 [(\alpha \pm \beta)/2] \quad \text{(hyperbola)} \tag{1.5.12}$$

Our analytical and geometrical results are consistent —that is, to each value of a, there correspond two ellipses or two hyperbolas that satisfy the requirements of the problem. Furthermore, in the elliptical case the conditions for minimum energy, as expressed by Eq. (1.2.2), imply $\alpha = \pi$ in Eq. (1.5.7). Also, since

$$0 \leq \beta \leq \alpha \leq \pi$$

it follows that

$$\sin^2 [(\alpha + \beta)/2] \geq \sin^2 [(\alpha - \beta)/2]$$

Therefore, if l_+ and l_- are used to denote the two roots given by Eq. (1.5.9), in accordance with the particular choice of sign, we have

$$l_+ \geq l_-$$

Since the distance L between the foci of an ellipse may be written as

$$L = 2\sqrt{a(a - l)}$$

it follows that $L_+ \leq L_-$

with the subscripts having the obvious interpretation. Therefore, in Eq. (1.5.9), the upper sign corresponds to the focus F^*, shown in Fig. 1-4, while the lower sign corresponds to the focus $\bar{F}^*$.

Similarly, in the hyperbolic case,

$$0 \leq \beta \leq \alpha$$

so that

$$\sinh^2 [(\alpha + \beta)/2] \geq \sinh^2 [(\alpha - \beta)/2]$$

Again denoting by l_+ and l_- the two roots given by Eq. (1.5.12), we have

$$l_+ \geq l_-$$

as before. On the other hand, the distance L between the foci of a hyperbola is

$$L = 2\sqrt{a(a + l)}$$

so that

$$L_+ \geq L_-$$

Therefore, in Eq. (1.5.12), the upper sign corresponds to the focus F^*, shown in Fig. 1-5, while the lower sign corresponds to the focus $\bar{F}^*$.

We may check our general formula for the latus rectum with the special results obtained previously by geometrical arguments. For example, in the minimum-energy case, where $a_m = s/2$, we have

$$\alpha_m = \pi, \quad \sin(\beta_m/2) = \sqrt{(s - c)/s}$$

Substitution into Eq. (1.5.9) produces the same expression for l_m as obtained in Eq. (1.2.5). The two roots normally obtained are identical, showing that only one minimum-energy path exists from P to Q.

For the case of the symmetrical ellipse in which, from Eq. (1.2.9),

$$a_s = (r_1 + r_2)/2 = (2s - c)/2$$

we see at once that the corresponding values of α and β are such that

$$\alpha_s + \beta_s = \pi$$

Eq. (1.2.10) for l_s follows immediately from the general expression for l if we choose the upper sign in Eq. (1.5.9).

We shall close this discussion by making one final observation. By using Eqs. (1.5.7) and (1.5.8), we may expand Eq. (1.5.9) as

$$l = [4(s - r_1)(s - r_2)/c^2] \times \{\sqrt{s/2}\sqrt{1 - [(s - c)/2a]} \pm \sqrt{1 - (s/2a)}\sqrt{(s - c)/2}\}^2$$

and determine the limit of l as a becomes infinite. Referring to Eqs. (1.4.1) and (1.4.2), we see at once that

$$\lim_{a \to \infty} l_+ = l_1, \quad \lim_{a \to \infty} l_- = l_2$$

which shows that the parabolic paths from P to Q are the limiting forms of elliptical paths with infinite major axes. A similar expansion of Eq. (1.5.12) and subsequent determination of the limit for increasing a also shows these same parabolas as the limiting forms of hyperbolas with infinite major axes.

Finally, one may consider, from an analytic point of view, the shape of the limiting hyperbolas as a approaches zero. By calculating the limiting slope of the asymptotes

$$\lim_{a \to 0} (b^2/a^2) = \lim_{a \to 0} (l/a)$$

the results stated at the end of Section (1.3) may be verified.

(1.6) *Time of Flight for a Conic Trajectory*

There are many interesting and sometimes surprising properties of conic trajectories. For example, one would scarcely anticipate that the period P of elliptic motion would depend only upon the major axis of the ellipse and not at all upon the eccentricity. The precise relationship is

$$P = 2\pi\sqrt{a^3/\mu} \qquad (1.6.1)$$

where a is the semi-major axis of the ellipse and μ is a constant of such a value that μ/r^2 gives the magnitude of the force at a distance r from the center of force.

The fact that a particle moving in free fall along a conic trajectory has a velocity magnitude V at any point that is a function only of the distance r from the center of force and the major axis is another example of one of the more interesting properties of conics. Here, again, nc dependence upon eccentricity is involved and the velocity is determined accordingly by

$$V^2 = \mu[(2/r) - (1/a)] \quad \text{(ellipse)} \qquad (1.6.2)$$

$$V^2 = \mu[(2/r) + (1/a)] \quad \text{(hyperbola)} \qquad (1.6.3)$$

$$V^2 = 2\mu/r \quad \text{(parabola)} \qquad (1.6.4)$$

Perhaps the most remarkable theorem in this connection was the one originally discovered by Lambert, and subsequently proved analytically by Lagrange, having to do with the time to traverse an elliptic arc under conditions of free fall. Lambert showed that this time depends only upon the length of the major axis, the sum of the distances of the initial and final points of the arc from the center of force, and the length of the chord joining these points. (Actually, the theorem is true for a general conic.) In terms of our notation, if T is the time to describe the arc from P to Q shown in Fig. 1-7, then Lambert's theorem states that

$$T = T(a, r_1 + r_2, c) \qquad (1.6.5)$$

We are again astonished to find that the ellipticity is not involved.

In this paper we shall not be concerned with a demonstration of the truth of Lambert's result, but will instead exploit an idea suggested by Lagrange to arrive at the precise analytical form of the functional relationship implied in Eq. (1.6.5). Since we have already seen that there are two paths from P to Q for each conic having the same values of a, r_1, r_2, and c, we must expect to find two different analytical expressions—one valid for each of the two paths.†

Consider first an elliptical arc from P to Q and, more

† For an ellipse connecting the points P and Q, there is, of course, a choice between two paths, according to whether the ellipse is traversed in the clockwise or counterclockwise direction. In our calculation of the time of flight T, we shall always assume counterclockwise motions from P to Q. The time to traverse the clockwise path may be obtained by subtracting T from the total period.

specifically, one whose vacant focus F^* lies along the lower branch of the hyperbolic locus shown in Fig. 1-4. Since the time T to traverse this arc does not depend on the eccentricity, we may consider instead the arc of a very flat ellipse, obtained by letting ϵ approach unity in such a way that a, $r_1 + r_2$, and c remain unchanged. Then, according to Eq. (1.6.5), the time to traverse the original arc subtended by the chord c and the time to traverse the corresponding arc of the flattened ellipse are the same. In this limiting process, as ϵ tends to unity with a fixed, the foci move out to the extremities of the ellipse and the entire curve flattens out to coincide with the major axis in the limit. Various stages, as the limit is approached, are shown in Fig. 1-8. The same time is required to traverse each of the three elliptical arcs shown in the Figure. Although the straight-line distance from P to Q remains constant, the distances of P and Q from the attractive focus will change, but in such a way that $PF + QF$ is invariant.

In the limit, the trajectory is rectilinear, the arc in question coincides exactly with the chord c, and we may compute the time T by elementary methods. To this end, we use Eq. (1.6.2) in the form

$$V^2 = (dr/dt)^2 = \mu[(2/r) - (1/a)]$$

since now all motion takes place along a straight-line path. Rewriting the preceding equation, we have

$$dt = (1/\sqrt{\mu})[r\, dr/\sqrt{2r - (r^2/a)}]$$

From Fig. 1-8(c), the end points of the arc P and Q are so located that

$$PF = (r_1 + r_2 - c)/2 = s - c$$

$$QF = (r_1 + r_2 + c)/2 = s$$

Hence,

$$T = (1/\sqrt{\mu}) \int_{s-c}^{s} [r\, dr/\sqrt{2r - (r^2/a)}]$$

Introducing the auxiliary quantities α and β, defined by Eqs. (1.5.7) and (1.5.8), and making the following change in the variable of integration:

$$r = a(1 - \cos \psi)$$

we have, finally,

$$T = \sqrt{a^3/\mu} \int_{\beta}^{\alpha} (1 - \cos \psi) d\psi$$

which becomes

$$T = (P/2\pi)[(\alpha - \sin \alpha) - (\beta - \sin \beta)] \quad \text{(ellipse)} \quad (1.6.6)$$

after performing the simple quadrature and introducing the period P defined in Eq. (1.6.1).

We now derive a corresponding expression for the time $\tilde{T}$ when the elliptical arc from P to Q has its vacant focus $\tilde{F}^*$ along the upper branch of the hyperbolic locus in Fig. 1-4. In this case, the chord c intersects the line connecting the two foci F and $\tilde{F}^*$ and this characteristic must be preserved when we pass to the limit of a very flat ellipse. This situation is illustrated in Fig. 1-9

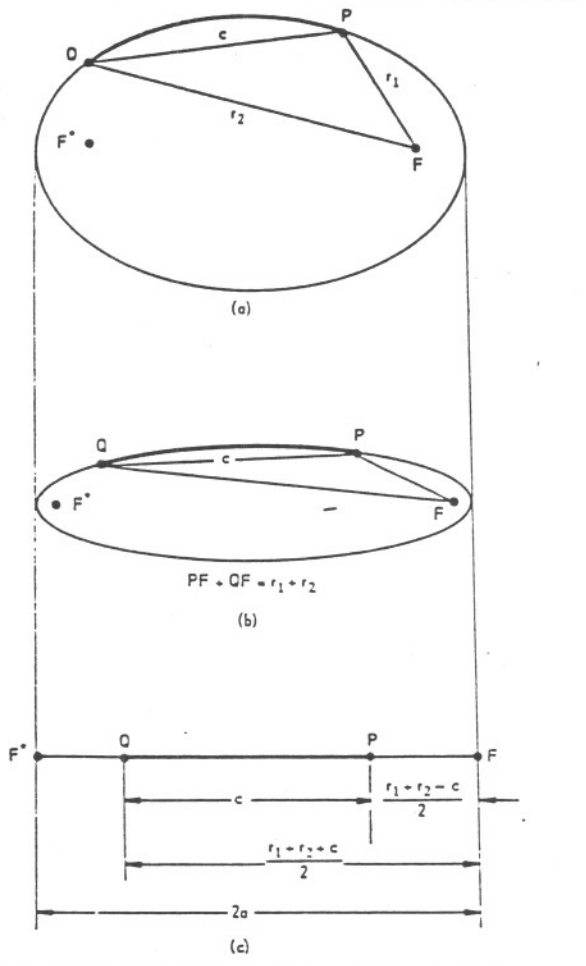

FIG. 1-8. Illustration of the significance of Lambert's theorem.

for various stages as ϵ tends to unity. In the limit, the time $\tilde{T}$ is then identical to the time to traverse the flattened ellipse from P to F^* and from F^* back to Q. Thus, to obtain $\tilde{T}$, we simply add to T twice the time to traverse the distance F^*Q; i.e.,

$$\tilde{T} = T + (2/\sqrt{\mu}) \int_{s}^{2a} [r\, dr/\sqrt{2r - (r^2/a)}]$$

$$= T + 2\sqrt{a^3/\mu} \int_{\alpha}^{\pi} (1 - \cos \psi) d\psi$$

Hence,

$$\tilde{T} = P - (P/2\pi)[(\alpha - \sin \alpha) + (\beta - \sin \beta)] \quad \text{(ellipse)} \quad (1.6.7)$$

For the case of the minimum-energy path, Eqs. (1.6.6) and (1.6.7) produce identical results. We have

$$T_m = \tilde{T}_m = (P_m/2\pi)[\pi - (\beta_m - \sin \beta_m)]$$

where

$$P_m = \pi\sqrt{s^3/2\mu}, \quad \sin(\beta_m/2) = \sqrt{(s - c)/s}$$

For the symmetrical ellipse, the time-of-flight expression is particularly simple. We have

$$T_s = (P_s/2\pi)(2\alpha_s - \pi) = (P_s/2\pi)(\pi - 2\beta_s)$$

where

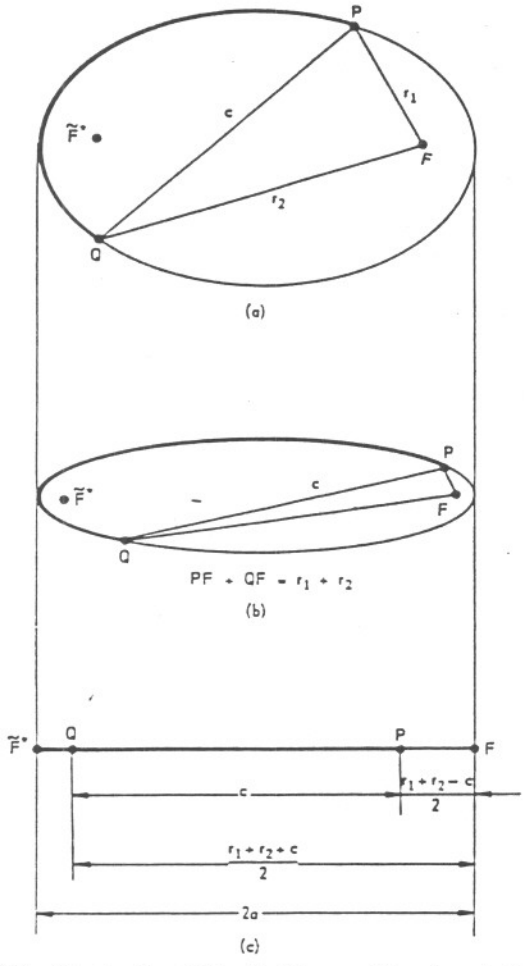

FIG. 1-9. Illustration of the significance of Lambe rt's theorem.

$$P_s = \pi\sqrt{(r_1 + r_2)^3/2\mu}$$

$$\cos\beta_s = -\cos\alpha_s = c/(r_1 + r_2)$$

Exactly the same technique may be used to obtain an analytic expression for the time to traverse a hyperbolic arc. Consider first a hyperbola connecting the points P and Q whose vacant focus F^* lies along the upper branch of the hyperbolic locus shown in Fig. 1-5. To compute the time T to traverse this arc, we again let ϵ approach unity in such a way that a, $r_1 + r_2$, and c remain unchanged. In the limit, when the trajectory is rectilinear, we may use Eq. (1.6.3) to obtain

$$T = (1/\sqrt{\mu}) \int_{s-c}^{s} [r\,dr/\sqrt{2r + (r^2/a)}]$$

If we introduce the auxiliary quantities α and β, defined by Eqs. (1.5.10) and (1.5.11), and make the following change in the variable of integration:

$$r = a(\cosh\psi - 1)$$

we find

$$T = \sqrt{a^3/\mu}\,[(\sinh\alpha - \alpha) - (\sinh\beta - \beta)]$$
(hyperbola) (1.6.8)

The hyperbolic trajectory, whose vacant focus F^* lies along the lower branch of the hyperbolic locus in Fig. 1-5, is characterized by the fact that the center of force F is contained in the area bounded by the chord c and the arc that it subtends. This characteristic must be preserved when passing to the limit. The time $\tilde{T}$ is then computed as the time to traverse the flattened hyperbola from P to F and from F to Q; i.e.,

$$\tilde{T} = T + (2/\sqrt{\mu}) \int_{0}^{s-c} [r\,dr/\sqrt{2r + (r^2/a)}]$$

Hence,

$$\tilde{T} = \sqrt{a^3/\mu}\,[(\sinh\alpha - \alpha) + (\sinh\beta - \beta)]$$
(hyperbola) (1.6.9)

We have seen, in our earlier discussions, that the parabolic trajectories from P to Q may be considered as limiting cases of either elliptic or hyperbolic trajectories with infinite major axes. If we compute the limit of T and $\tilde{T}$ as a becomes infinite, we should obtain the times T_1 and T_2 to traverse the parabolic arcs shown in Fig. 1-6. Indeed, from Eqs. (1.6.8) and (1.6.9) we find

$$T_1 = \lim_{a\to\infty} T = (1/3)\sqrt{2/\mu}\,[s^{3/2} - (s-c)^{3/2}]$$
(parabola) (1.6.10)

$$T_2 = \lim_{a\to\infty} \tilde{T} = (1/3)\sqrt{2/\mu}\,[s^{3/2} + (s-c)^{3/2}]$$
(parabola) (1.6.11)

The same expression for T_1 in Eq. (1.6.10) may also be obtained using Eq. (1.6.6). On the other hand, the parabola PV_2Q of Fig. 1-6 corresponds, in the limit of increasing a, to the lower branch of the elliptical arc with vacant focus $\tilde{F}^*$. Thus, to produce the formula for T_2 from the time-of-flight expression for an elliptical arc, we must use the complementary form of Eq. (1.6.7) obtained by subtracting T of that equation from the period P.

(2) Interplanetary Trajectories in a Simple Model of the Solar System

(2.1) *Departure Velocity From a Circular Orbit*

Of fundamental importance to the problem of planetary reconnaissance is the impulse in velocity needed in order that a spaceship may attain a suitable interplanetary orbit. In the present section we shall analyze these velocity requirements using a simplified model of the solar system. The basic assumptions will be that the planets describe circular orbits around the sun and that the planes of these orbits are situated in the plane of the ecliptic. Later, in Section (3), we shall consider the more complex model in which the planetary orbits are elliptical and are inclined with respect to the plane of the ecliptic. Furthermore, we shall not consider here the problem of launching a vehicle from the surface of a planet. We assume, instead, that our interplanetary voyage begins at a point that is sufficiently far removed from the gravitational field of the planet that we need consider only the attraction of the sun. The vehicle or spaceship has

an initial velocity that is the same as the orbital velocity of the planet of departure. Our problem will be to determine the additional velocity required to place the spaceship in an orbit that intersects the orbit of the destination planet at a predetermined point in space.

As the first step in our analysis, we will derive expressions for the polar-coordinate components of the velocity of a vehicle moving in a conic trajectory. From the polar equation for a general conic,

$$r = l/(1 + \epsilon \cos \phi) \tag{2.1.1}$$

we obtain

$$dr/dt = [\epsilon \sin \phi/(1 + \epsilon \cos \phi)]\, r(d\phi/dt)$$

from which it follows that

$$(dr/dt)^2 + [r(d\phi/dt)]^2 = [\epsilon^2 - 1 + 2(l/r)](r^2/l^2)[r(d\phi/dt)]^2$$

But,
$$\epsilon^2 - 1 = \begin{cases} -(l/a) & \text{(ellipse)} \\ 0 & \text{(parabola)} \\ l/a & \text{(hyperbola)} \end{cases}$$

$$(dr/dt)^2 + [r(d\phi/dt)]^2 = (2\mu/r) + \begin{cases} -(\mu/a) & \text{(ellipse)} \\ 0 & \text{(parabola)} \\ \mu/a & \text{(hyperbola)} \end{cases}$$

Hence,

$$[r(d\phi/dt)]^2 = \mu l/r^2 \tag{2.1.2}$$

$$(dr/dt)^2 = \mu[(2r - l)/r^2] + \begin{cases} -(\mu/a) & \text{(ellipse)} \\ 0 & \text{(parabola)} \\ \mu/a & \text{(hyperbola)} \end{cases} \tag{2.1.3}$$

In order to keep the energy requirements within reasonable bounds, we shall restrict our discussion of departure velocities for orbital transfer missions to those required for elliptical trajectories.

Refer to Fig. 2-1 and consider a spaceship in a circular orbit of radius r_1 about a center of attraction. The orbital velocity V_0 is

$$V_0^2 = \mu/r_1 \tag{2.1.4}$$

When the vehicle is at the point P, a velocity increment V_R is applied in such a way that the ship will leave its present orbit at P with velocity V_P and move along an elliptical trajectory to a point Q at a distance r_2 from the center of force. We wish to determine the velocity increment V_R as a function of the heliocentric angle θ through which the ship moves in its voyage from P to Q. In particular, we are interested in the minimum velocity required for any given mission.

After the velocity increment V_R is applied, the ship will have a velocity V_P whose polar components $(dr/dt)_P$ and $(rd\phi/dt)_P$ are obtained from Eqs. (2.1.2) and (2.1.3). Since V_R is defined by

$$V_R^2 = (dr/dt)_P^2 + \{[r(d\phi/dt)]_P - V_0\}^2$$

we may use Eq. (2.1.4) to obtain

$$V_R^2 = V_0^2[3 - (r_1/a) - 2\sqrt{l/r_1}] \tag{2.1.5}$$

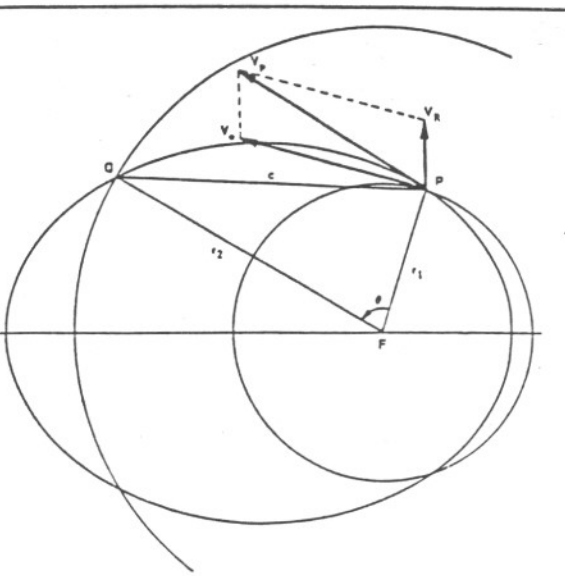

FIG. 2-1. Velocity requirements for an orbit to orbit voyage

Let us introduce the dimensionless quantity

$$\Delta E = V_R^2/V_0^2$$

which is a measure of the amount of energy needed at point P to transfer from a circular orbit to an elliptical orbit for a voyage to Q. Then, from Eq. (1.5.9) and a simple trigonometric identity, we have

$$\Delta E = 3 - (r_1/a) - 4(\sqrt{ar_2}/c) \times \sin(\theta/2) \sin[(\alpha \pm \beta)/2] \tag{2.1.6}$$

Using the definitions of α and β given by Eqs. (1.5.7) and (1.5.8), we may write ΔE in an alternate form as

$$\Delta E = 3 - (r_1/a) - (r_2\sqrt{2r_1}/c) \times \sin\theta\{\sqrt{[1/(s-c)] - (1/2a)} \pm \sqrt{(1/s) - (1/2a)}\} \tag{2.1.7}$$

From an examination of the derivative

$$\frac{d(\Delta E)}{da} = \frac{r_1}{a^2}\left[1 - \frac{r_2 \sin\theta}{2c\sqrt{2r_1}}\left(\frac{1}{\sqrt{[1/(s-c)] - (1/2a)}} \pm \frac{1}{\sqrt{(1/s) - (1/2a)}}\right)\right] \tag{2.1.8}$$

and Eq. (2.1.7), we note the following:

(a) ΔE is a double-valued function of a having an infinite slope at $a = a_m = s/2$, the smallest value of a for which an elliptical path from P to Q is possible.

(b) If we denote by ΔE_+ and ΔE_- the two branches of the function ΔE corresponding respectively to the upper and lower signs in Eq. (2.1.7), we see that

$$\Delta E_+ \leq \Delta E_-$$

with equality obtaining only when $a = a_m$.

(c) As a increases, ΔE approaches asymptotically the values

$$3 - (r_2\sqrt{2r_1}/c) \sin\theta[(1/\sqrt{s-c}) \pm (1/\sqrt{s})]$$

(d) The slope of the upper branch ΔE_- is always positive, while the slope of the lower branch ΔE_+ is negative

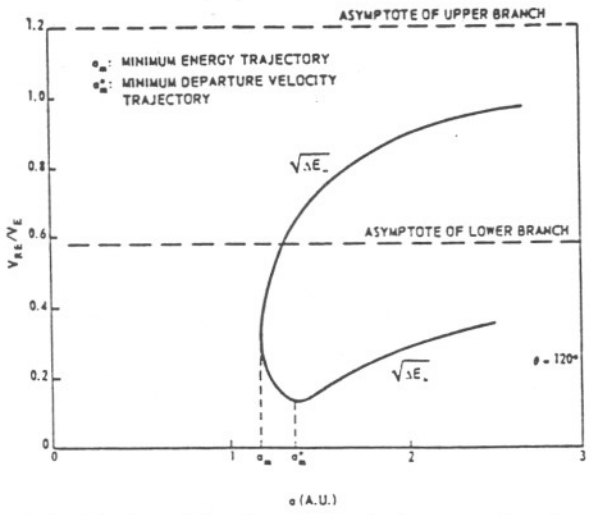

FIG. 2-2. Earth to Mars departure velocity vs. semi-major axis of transfer ellipse for $\theta = 120°$.

for a near a_m. The possibility that ΔE_+ will have a minimum for a finite value of a will be considered in the following section.

A graph of the function $\sqrt{\Delta E}$ versus a is provided in Fig. 2-2. The selected mission is a voyage from Earth to Mars, so that r_1 and r_2 are chosen, respectively, as the mean distances of the planets from the sun. The heliocentric angle θ traveled was taken as 120° for purposes of illustration. The ordinate V_{RE}/V_E shows directly the additional velocity that must be provided for the trip as a fraction of the Earth's orbital velocity. Since the Earth's velocity is almost 100,000 ft. per sec., the approximate conversion of V_{RE} into units of feet per second is immediate. The abscissa a is shown as a multiple of the astronomical unit (A.U.).

(2.2) *Minimum Departure Velocity From a Circular Orbit*

The minimum-energy trajectory discussed in Section (1) should not be confused with the trajectory requiring the minimum departure velocity. Indeed, for the particular case illustrated in Fig. 2-2, the additional velocity in excess of the orbital velocity needed to travel the minimum-energy path ($a = a_m$) is about double the minimum departure velocity. As a matter of fact, the only trajectory that minimizes both the velocity relative to the sun and the velocity relative to the planet of departure is the so-called Hohmann ellipse. The Hohmann orbit is distinguished as being co-tangential to the orbit of the planet of departure and to the orbit of the destination planet.

The energy requirements for the Hohmann path cannot be obtained directly from Eq. (2.1.7). The polar angle θ is equal to π and Eq. (2.1.7) is indeterminate for this value. However, because of the simplicity of the geometry, we may evaluate the elements of the Hohmann ellipse directly and then use Eq. (2.1.5) to determine the energy requirements ΔE.

The points of departure and arrival for a Hohmann trajectory correspond, respectively, to perihelion and aphelion. Thus, if a_H, l_H, and ϵ_H, are, respectively, the semi-major axis, semi-latus rectum and eccentricity, we have

$$a_H(1 - \epsilon_H) = r_1, \quad a_H(1 + \epsilon_H) = r_2$$

so that†

$$a_H = [(r_1 + r_2)/2], \quad l_H = 2[r_1r_2/(r_1 + r_2)]$$

Finally, from Eq. (2.1.5), we have

$$\Delta E_H = 3 - [2r_1/(r_1 + r_2)] - 2\sqrt{2r_2/(r_1 + r_2)} \quad (2.2.1)$$

The Hohmann trajectory is not necessarily the ideal one for interplanetary travel. The precise orientation of the departure and destination planets that is required for the Hohmann path is one obvious disadvantage. Another, to be discussed in Section (3), results from the three-dimensional nature of the solar system. Its chief interest, therefore, lies in the fact that it provides, in our simple model, a lower bound for the energy requirements of any mission—i.e., for a fixed r_1 and r_2 we have

$$\Delta E_H \leq \Delta E$$

with equality obtaining only for $\theta = \pi$ and $a = (r_1 + r_2)/2$.

Obviously, in planning an interplanetary voyage, it is of advantage to be as flexible as possible with regard to the time of departure. Therefore, it is of interest to examine the energy requirements ΔE for an arbitrary configuration of the departure and destination planets. To this end, let us determine, for a fixed r_1, r_2, and θ, under what conditions ΔE, as defined in Eq. (2.1.7). has a minimum value.

It was noted in the previous section that the slope of the lower branch ΔE_+ of the ΔE curve is negative for values of a near a_m. Referring to Eq. (2.1.8), we see that ΔE_+ will have a positive slope if a value of a exists such that

$$\{1/\sqrt{[1/(s - c)] - (1/2a)}\} + [1/\sqrt{(1/s) - (1/2a)}] < 2c\sqrt{2r_1}/r_2 \sin\theta$$

Clearly, the difference between the left-hand side of the preceding inequality and $\sqrt{s - c} + \sqrt{s}$ can be made arbitrarily small by choosing a to be sufficiently large. Thus, we are led to determine the conditions under which the inequality

$$\sqrt{s - c} + \sqrt{s} < 2c\sqrt{2r_1}/r_2 \sin\theta \quad (2.2.2)$$

holds. For this purpose, we note that

$$(\sqrt{s - c} + \sqrt{s})^2 = 2\sqrt{r_1r_2}\cos(\theta/2) + r_1 + r_2 \leq (\sqrt{r_1} + \sqrt{r_2})^2$$

and

$$(2c\sqrt{2r_1}/r_2 \sin\theta)^2 \geq 8r_1$$

Hence, a sufficient condition for E_+ to possess a minimum is that

† If we compare these results with Eqs. (1.2.2), (1.2.5), (1.2.6), (1.2.7), (1.2.9), and (1.2.10), we see that the Hohmann orbit, the minimum-energy ellipse, the osculating ellipse, and the symmetrical ellipse are all identical for $\theta = \pi$.

$$\sqrt{r_1} + \sqrt{r_2} < 2\sqrt{2r_1} \qquad (2.2.3)$$

If $r_2 < r_1$, the condition of Eq. (2.2.3) holds. Therefore, an elliptical path, requiring minimum departure velocity, to an inner planet always exists. Furthermore, one sees that this condition holds also for a trip from Earth to Mars. On the other hand, for the remainder of the outer planets, the inequality does not hold and one might expect to find values of θ for which the minimum departure velocity trajectory is parabolic. As a matter of fact, this rather surprising condition does prevail for Jupiter and the planets beyond. One should note, however, that the condition of Eq. (2.2.2) can always be satisfied if $\sin\theta$ is made small enough. Thus, for the outer planets there are sectors near $\theta = 0$ and $\theta = \pi$ for which minimum-departure-velocity elliptical trajectories exist. However, the farther from the sun, the smaller these sectors become.

The value of a for which ΔE_+ attains its minimum value (assuming that one exists) is obtained as the root of the equation

$$\{1/\sqrt{[1/(s-c)] - (1/2a)}\} + [1/\sqrt{(1/s) - (1/2a)}] = 2c\sqrt{2r_1}/r_2 \sin\theta \qquad (2.2.4)$$

which, after reduction to a normal form, is found to be of fourth degree in a. For practical purposes, the solution of Eq. (2.2.4) is obtained more easily as follows. First, rewrite the equation in the equivalent form

$$\{1/\sqrt{(1/s) - (1/2a) + [c/s(s-c)]}\} + [1/\sqrt{(1/s) - (1/2a)}] = 2c\sqrt{2r_1}/r_2 \sin\theta$$

and then introduce a new variable ζ defined by

$$\tan\zeta = \sqrt{(1/s) - (1/2a)}/\sqrt{c/s(s-c)}, \qquad 0 \le \zeta < \pi/2 \qquad (2.2.5)$$

so that Eq. (2.2.4) becomes

$$\cos\zeta + \cot\zeta = (2c/r_2 \sin\theta)\sqrt{2cr_1/s(s-c)}$$

or, alternately,

$$\cos\zeta + \cot\zeta = 4(c/r_2)^{3/2}/\sin\theta\sqrt{1+\cos\theta} \qquad (2.2.6)$$

Eq. (2.2.6) may be solved for ζ almost by inspection, using a table of trigonometric functions. With this value of ζ, Eq. (2.2.5) may be solved for the corresponding major axis $2a_m^*$. Thus, we obtain

$$2a_m^* = \frac{r_1 r_2(1+\cos\theta)}{r_1 + r_2 - c(\sec^2\zeta + \tan^2\zeta)} \qquad (2.2.7)$$

Finally, the energy change ΔE_m^* needed for this trajectory is found by substitution into Eq. (2.1.7). We have, after some simplification,

$$\Delta E_m^* = 3 - 2\frac{r_1 + r_2 - c[(\sec\zeta - \tan\zeta)^2 - 2\sec\zeta\tan\zeta]}{r_2(1+\cos\theta)} \qquad \text{(finite } a_m^*\text{)} \qquad (2.2.8)$$

When ΔE_+ is a monotonically decreasing function of a, the minimum value occurs for infinite a. The trajectory is parabolic and

$$\Delta E_m^* = 3 - (2r_2/c)\sin\theta[\sqrt{r_1/(r_1+r_2-c)} + \sqrt{r_1/(r_1+r_2+c)}] \quad \text{(infinite } a_m^*\text{)} \qquad (2.2.9)$$

For the special case in which $\theta = \pi$, the trajectory is of the Hohmann type and the minimum value of ΔE_+ is ΔE_H, as obtained from Eq. (2.2.1).

Fig. 2-3 gives plots of $(V_{R\mathcal{E}}/V_{\mathcal{E}})_m^* = \sqrt{\Delta E_m^*}$ as a function of θ for a voyage from Earth to each of the other planets of the solar system. The curves for the two most remote planets, Neptune and Pluto, are not shown because, with the scale used, they would be indistinguishable from the curve for Uranus. The sections of the curves for Jupiter, Saturn, and Uranus, corresponding to parabolic trajectories as the minimum-velocity paths, are characterized by broken lines.

(2.3) *Nonstop Round-Trip Interplanetary Trajectories*

Consider, as a specific mission for an interplanetary voyage, placing a spaceship in an orbit that passes within a few thousand miles of another planet and subsequently returns to Earth. The problem of determining a suitable one-way trajectory may be solved with relative ease, using the material thus far developed. The added complication of requiring the vehicle to return to Earth without additional propulsion (except that needed to correct for navigational inaccuracies) would not contribute significantly to the difficulty of obtaining a solution were it not for the deflection of the orbit caused by the gravitational field of the planet as the spaceship passes. Before treating the effect of perturbations introduced by the destination planet, let us consider first the nonstop round-trip trajectory, with the sun as the only gravitational force affecting the orbit.

The simplest possible round-trip trajectory would be an orbit whose period is a multiple of the Earth's period. For purposes of illustration and to obtain an

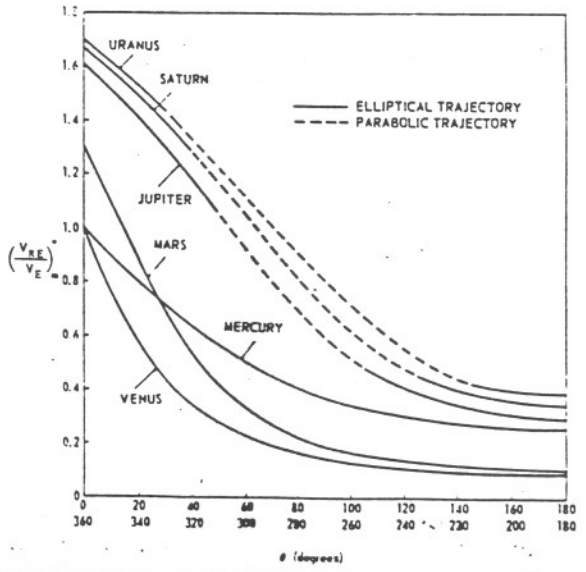

FIG. 2-3. Minimum departure velocity as a function of polar angle θ.

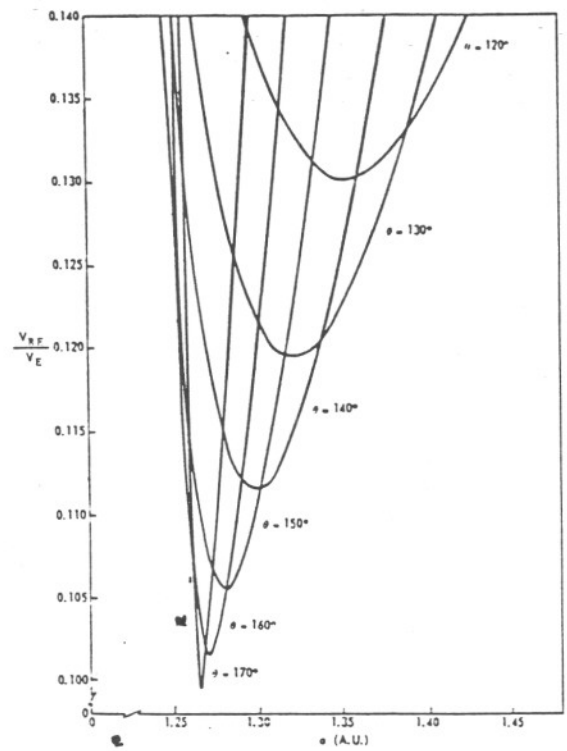

FIG. 2-4. Earth to Mars departure velocity vs. semi-major axis of transfer ellipse for various values of the polar angle θ.

appreciation for the magnitude of the velocities involved, let us investigate the possibilities of a spaceship orbit with a period of one year, that intersects the orbits of both Earth and Mars. From Eq. (1.6.1) we see that the semi-major axis a of such an orbit must be the same as that for the Earth—i.e., one astronomical unit (A.U.). Since the smallest value that a can assume is that for minimum energy, we find, from Eq. (1.2.2), that the largest possible linear distance between the point of departure and the first crossing of the Martian orbit is 1.48 A.U., assuming the radius of the Martian orbit to be 1.52 A.U. Therefore, the spaceship must reach the Martian orbit after traversing an angular distance θ of not more than about 68.3°. From Eq. (2.1.7), we see that, for a one-year orbit and for the maximum possible value of θ, the required departure velocity is approximately 61,000 ft. per sec. Orbits with a one-year period requiring less velocity do exist for smaller values of θ; however, from the curves shown in Fig. 2-3, we see at once that this possibility ceases for angles less than about 35°. For example, we need a velocity of some 53,600 ft. per sec. for $\theta = 58°$; but, for $\theta = 48°$, the required velocity for a one-year orbit is more than 95,400 ft. per sec.

The velocity requirements for an orbit whose period is 1.5 years are considerably more relaxed. In this case, the spaceship makes two circuits of the sun while the Earth makes three. The necessary semi-major axis is about 1.31 A.U. and calculations similar to the preceding show that such an orbit is possible for any value of θ. In Fig. 2-4, the lower portions of the Earth-to-Mars departure-velocity curves, as a function of the semi-major axis of the associated ellipse, are plotted for various values of θ. From these curves, we see explicitly how the velocity requirements for a 1.5-year orbit depend upon the polar angle θ. The minimum departure velocity for such a trajectory is approximately 11,200 ft. per sec. and the corresponding value for θ is about 142°. Fig. 2-5 gives the time of flight from Earth to Mars as a function of the semi-major axis, plotted for several values of θ. From these curves, the time to reach Mars on the minimum-departure-velocity trajectory having a 1.5-year period is seen to be approximately 185 days.

It is, of course, possible to have round-trip orbits that return to Earth after a non-integral number of years. However, we shall not pursue this point further before considering the additional effect of disturbances induced by the destination planet.

The perturbations experienced by the orbit of a spaceship, when in the vicinity of a planet, depend upon the relative velocity with which the vehicle overtakes or is overtaken by the planet and the distance separating the two at the point of closest approach. In the absence of any gravitational fields other than the planet's own, the spaceship would approach the planet along a hyperbolic path. At a sufficiently great distance the motion would be essentially along the asymptote and would have a velocity V_∞ relative to the planet given by

$$V_\infty^2 = \mu_P / a_h$$

according to Eq. (1.6.3). Here, we have denoted the semi-major axis of the hyperbola by a_h and the gravitational constant of the planet by μ_P.

Referring to Fig. 2-6, we define δ to be the angle between the asymptote and the conjugate axis of the hyperbolic path of approach, ϵ_h to be the eccentricity of the orbit, D the distance between the vertex and the

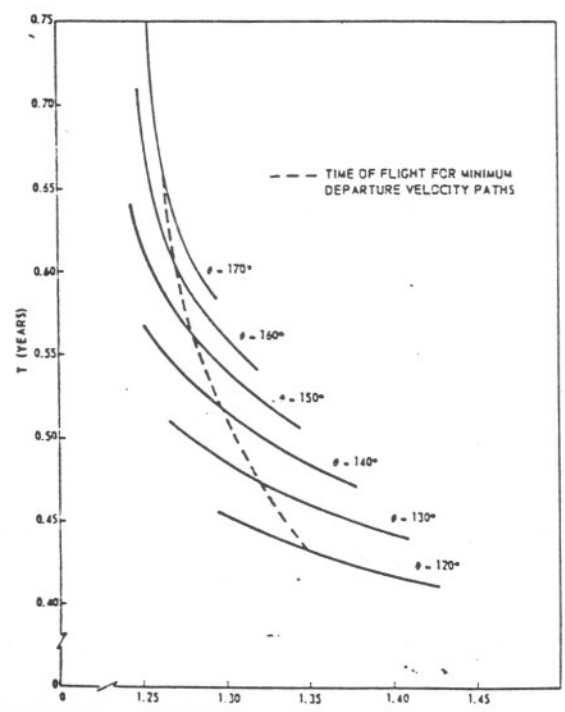

FIG. 2-5. Earth to Mars time of flight vs. semi-major axis of transfer ellipse for various values of the polar angle θ.

focus, and d the distance between the vertex and the surface of the planet. The vertex is, of course, the point of closest approach of the spaceship to the planet, and we have the relationship

$$D = a_h(\epsilon_h - 1) = (\mu_P/V_\infty^2)(\epsilon_h - 1)$$

Solving for ϵ_h and noting that $\epsilon_h = \csc \delta$ we obtain

$$\sin \delta = 1/[1 + (DV_\infty^2/\mu_P)] \qquad (2.3.1)$$

Therefore, the total effect on the velocity of the spaceship, after contact with a planet, is simply a rotation in the plane of motion of the relative component of velocity by an amount 2δ. The direction of rotation of the relative velocity vector will tend to increase or decrease the absolute velocity according to whether the spaceship passes behind or ahead of the planet, respectively.

The mass ratio of the sun to Mars is 3,093,500. Therefore, the attraction of the planet does not become as large as one hundredth of the attraction of the Sun until the spaceship is within about 800,000 miles of Mars. By a direct calculation, using Eqs. (1.5.9), (2.1.2), and (2.1.3), we find that a vehicle moving in a 1.5-year orbit that intersects the Martian orbit at $\theta = 140°$ has a velocity component in the direction of the motion of Mars of about 48,800 m.p.h. and a radial component away from the sun of approximately 8,770 m.p.h. Since the orbital velocity of Mars is about 54,000 m.p.h., the spaceship is being overtaken by the planet and the relative velocity between the two bodies is more than 10,000 miles per hour. Thus, the vehicle is within the critical 800,000-mile distance of the planet for less than 6.5 days. For other round-trip orbits, the relative velocity is higher, so that the period of time during which Mars can influence the orbit will be correspondingly smaller.

Because of the above considerations, it seems reasonable, as a good approximation to the true state of affairs, to view the effect of Mars on the trajectory as simply an impulse in velocity applied at the instant the spaceship crosses the Martian orbit. In computing the magnitude and direction of the velocity impulse, we shall use Eq. (2.3.1) to obtain the turn angle 2δ, with V_∞ taken as the relative velocity of the spaceship with respect to Mars, determined at the point of intersection of the two orbits.

Considering again the problem of a vehicle moving in a 1.5-year orbit that intersects the orbit of Mars at $\theta = 140°$, let us assume that the closest approach to the surface of the planet is 3,000 miles and that the ship passes ahead of Mars. Then, following the procedure outlined, the relative velocity is 10,245 m.p.h. and the turn angle 2δ is 23°. Therefore, the effect of the contact is to reduce the absolute velocity from 49,540 to 46,150 m.p.h. Furthermore, the period of the orbit is reduced from 1.5 to 1.31 years, as determined from Eqs. (1.6.2) and (1.6.1). These are, of course, sizeable changes, which must be taken into account in calculating round-trip interplanetary reconnaissance trajectories.

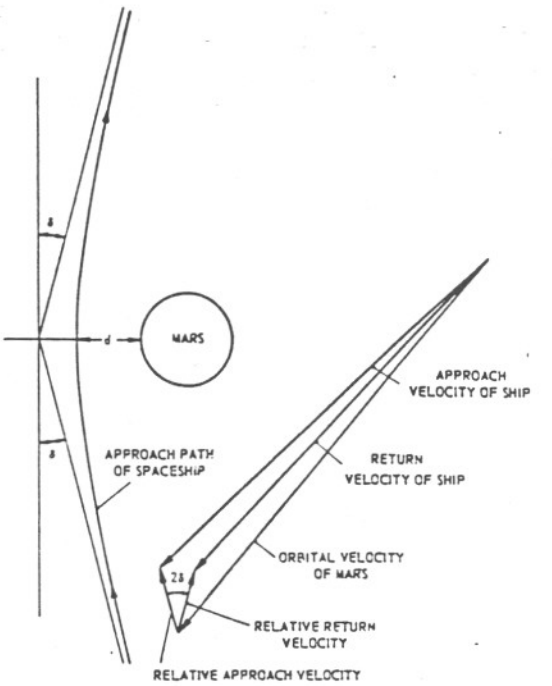

FIG. 2-6. Motion of spaceship in vicinity of Mars.

(2.4) *Reconnaissance Trajectories for the Planet Mars*

Using our simple model of the solar system, we shall now describe a method for computing nonstop trajectories from Earth to a planet and return. For definiteness, we shall choose the planet Mars as the target and consider, as allowable spaceship orbits, elliptical trajectories requiring reasonable departure velocities. The calculation technique to be described is not necessarily the most efficient considering the simplicity of our model; however, the ideas are readily adapted to the more difficult three-dimensional problem that will be treated in Section (3).

Let V_E be the orbital velocity of the Earth and let a departure velocity magnitude V_{RE} from the Earth's orbit be specified. We now choose a value θ_D for the heliocentric angle θ between the point of departure on the Earth's orbit and the point on the Martian orbit at which we intend to intercept Mars. Then, with $\Delta E = (V_{RE}/V_E)^2$ and $\theta = \theta_D$, Eq. (2.1.7)† is solved for the corresponding value of the semi-major axis a_D of the departure orbit. Obviously, a solution is not always possible. On the other hand, the equation may have two roots, each of which corresponds to a satisfactory solution to the problem of determining a departure orbit.

The next step in the procedure is to compute the time T required for the journey from Earth to Mars. For this purpose, we may use the following convenient formula, which is universally valid if θ is not an integral multiple of π. Thus, if we define N to be the integral

† Actually, Eq. (2.1.7) holds only for positive values of $\sin \theta$. Therefore, if θ lies in the third or fourth quadrant, we must use the symmetry inherent in our simple model—i.e., for any integer k, we observe that θ and $2k\pi - \theta$ require identical departure orbits for the same velocity.

part of $\theta/2\pi$, we may use Eqs. (1.6.6) and (1.6.7), together with the properties of symmetry, to show that

$$T = (P/2)\{2N + 1 + [\text{sgn}(\sin\theta)/\pi] \times [\pm(\alpha - \sin\alpha - \pi) - (\beta - \sin\beta)]\} \quad (2.4.1)$$

The positive or negative sign is used, respectively, according to whether the root a_D was obtained from the ΔE_+ branch of the curve or the ΔE_- branch. The function sgn is defined as $+1$, 0, or -1, according to whether the argument is, respectively, positive, zero, or negative.

With the time for the trip from Earth to Mars determined, the location of Mars at the time of departure is fixed. Thus, the orientations of the planets, and hence the time at which the voyage may start, is a consequence of the selected departure orbit.

The relative velocity V_{RM} of the spaceship with respect to Mars can be calculated at the point of intersection with the Martian orbit from the relationship

$$V_{RM}^2 = V_M^2[3 - (r_2/a_D) - 2\sqrt{l_D/r_2}] \quad (2.4.2)$$

where V_M is the orbital velocity of Mars and l_D is the semi-latus rectum of the departure orbit.

Setting aside for the moment the effect of Mars on the orbit, let us consider next the problem of returning to Earth. The procedure for determining an appropriate return trajectory that intersects the orbit of the Earth is the same as used in obtaining the departure trajectory. The magnitude of the relative velocity with which the ship leaves Mars is the same as that with which it arrived, regardless of the perturbations induced by the contact. Therefore, we may proceed as before by selecting the heliocentric angle θ_R measured from the intercept point on the Martian orbit to the point on the Earth's orbit where we may hope to reestablish contact with the Earth. Again, we use Eq. (2.1.7), with $\Delta E = (V_{RM}/V_M)^2$ and with r_1 and r_2 now taken as the radii of the orbits of Mars and Earth, respectively, to solve for the semi-major axis a_R of the return orbit. If a solution exists, Eq. (2.4.1) may be used as before to determine the time for the return trip.

With the time for the complete round trip known, it is a simple matter to determine the location of the Earth at the instant the spaceship returns to the orbit of the Earth. By systematically varying the choice of the angle θ_R and repeating the calculations just described, we will either find a return trajectory that contacts the Earth or conclude that none exists.

Assuming that a return trajectory has been found, it remains to determine whether the gravitational field of Mars is sufficient to accomplish the transfer of the spaceship from the departure orbit to the return orbit. Using Eqs. (2.1.2) and (2.1.3), we may compute the necessary angle 2δ through which the relative velocity vector must be rotated in order to change orbits. Then if V_{RM} is the magnitude of the relative velocity vector and μ_M is the gravitational constant of Mars, we may compute the required passing distance D from

$$D = (\mu_M/V_{RM}^2)(\csc\delta - 1) \quad (2.4.3)$$

If D has a reasonable value, considering the objectives of the reconnaissance mission, we will have a solution to the round-trip trajectory problem.

A digital computer program has been prepared that mechanizes the preceding computational procedure. By specifying the departure velocity and an angular increment used to generate values of θ_D, the computer will systematically find all of the corresponding round-trip trajectories. For purposes of illustration, the results of this program are summarized in Table 1 for a departure velocity equal to 0.13 times the Earth's orbital speed and an angular increment of 10°. Certain arbitrary bounds were placed on the program to prevent the computer from generating a trajectory requiring more than 3.5 years for the round trip or passing closer than 500 miles to, or farther than 30,000 miles from, the surface of Mars. The notation and units used in Table 1 are listed as follows:

- θ_D = heliocentric angle through which the spaceship moves from Earth to Mars, deg.
- a_D = semi-major axis of the departure ellipse, A. U.
- ϵ_D = eccentricity of the departure ellipse
- T_{EM} = time for trip from Earth to Mars, days
- V_{RM} = relative velocity of vehicle with respect to Mars at point of intersection with the Martian orbit, ft. per sec.
- 2δ = angle of rotation of the relative velocity vector resulting from contact with Mars, deg.

TABLE 1

Trip No.	θ_D, deg.	a_D, A.U.	ϵ_D	T_{EM}, days	V_{RM}, ft./sec.	2δ, deg.	d, miles	θ_R, deg.	a_R, A.U.	ϵ_R	T_{ME}, days	Δ_{EM}, deg.	T_{TOT}, years
1	130	1.379	0.275	164	20,300	8.5	6,600	528	1.297	0.301	869	44	2.828
2	130	"	"	"	"	6.7	9,100	632	1.314	0.296	974	"	3.115
3	230	"	"	428	"	17.3	1,800	434	1.228	0.333	612	6	2.846
4	230	"	"	"	"	11.3	4,300	563	1.274	0.311	742	"	3.203
5	490	"	"	756	"	14.3	2,300	283	1.250	0.322	393	−266	3.147
6	140	1.359	0.266	175	19,100	6.5	11,100	534	1.301	0.286	874	48	2.872
7	140	"	"	"	"	5.0	15,300	625	1.314	0.281	966	"	3.124
8	220	"	"	403	"	13.1	4,000	442	1.251	0.308	634	9	2.838
9	220	"	"	"	"	8.5	7,800	555	1.285	0.293	748	"	3.152
10	500	"	"	754	"	19.9	1,700	130	1.207	0.332	250	−255	2.750
11	500	"	"	"	"	10.4	5,800	275	1.271	0.299	397	"	3.152
12	210	1.234	0.255	375	17,400	7.5	11,500	455	1.278	0.278	665	14	2.846
13	510	"	"	751	"	9.8	8,100	157	1.262	0.285	291	−243	2.853
14	510	"	"	"	"	5.0	18,600	260	1.295	0.270	396	"	3.140

d = minimum passing distance from the surface of Mars, miles
θ_R = heliocentric angle through which the spaceship moves from Mars to Earth, deg.
a_R = semi-major axis of return ellipse, A.U.
ϵ_R = eccentricity of return ellipse
T_{ME} = time of trip from Mars to Earth, days
A_{EM} = heliocentric angle between Earth and Mars at instant of departure, in degrees measured in the counterclockwise direction from Earth to Mars
T_{TOT} = total time for the round trip, years

In Section (3), certain of these trajectories will be compared with their three-dimensional counterparts.

(3) Planetary Reconnaissance Trajectories in a Three-Dimensional Model of the Solar System

(3.1) *Coordinate Systems, Angles and Directions*

As a preliminary step in the development of a procedure for determining nonstop, round-trip planetary reconnaissance trajectories in a true model of the solar system, it will be convenient to introduce the various systems of coordinates that will be needed. Wherever possible we shall adopt the coordinate systems and notation that have been universally accepted in the field of celestial mechanics.

The position of the Earth at any time will be specified in terms of a set of heliocentric rectangular components. As shown in Fig. 3-1, the x and y axes are chosen in the plane of the ecliptic, with the positive x axis in the direction of the vernal equinox. The positive y axis is in the general direction of the perihelion of the Earth's orbit, and the z axis is chosen to make a right-handed coordinate system. Unit vectors in these three directions will be defined, respectively, as $\boldsymbol{i}_x$, $\boldsymbol{i}_y$, and $\boldsymbol{i}_z$.

The line of intersection of the plane of the Martian orbit with the plane of the ecliptic is called the line of nodes. The ascending node AN is the point at which Mars crosses the ecliptic with a positive component of velocity in the z direction. The longitude of the ascending node as measured from the vernal equinox will be denoted by Ω. The angle of inclination of the orbital plane of Mars to the ecliptic is called i.

To specify the location of Mars, a different set of heliocentric coordinates will be used. The ξ and η axes are selected in the Martian orbital plane with the positive ξ axis in the direction of the perihelion of the Martian orbit. The η and ζ axes are then chosen, as shown in Fig. 3-1, to make the system right-handed. Associated with the three axes are the unit vectors $\boldsymbol{i}_\xi$, $\boldsymbol{i}_\eta$, and $\boldsymbol{i}_\zeta$. The ξ axis makes an angle ω with the direction of the ascending node.

Let a_E, ϵ_E, and l_E be, respectively, the semi-major axis, the eccentricity, and the semi-latus rectum of the Earth's orbit, and correspondingly define a_M, ϵ_M, l_M for Mars. Furthermore, denote by Π_E and $\Pi_M = \Omega + \omega$ the respective longitudes of the perihelions of

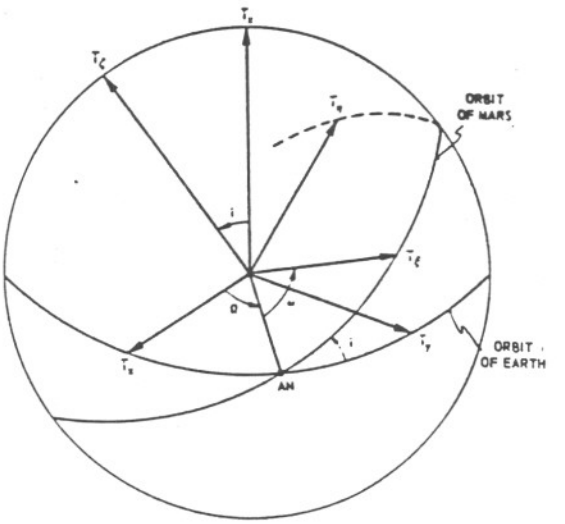

FIG. 3-1. Fixed heliocentric rectangular coordinates for Earth and Mars orbits.

the Earth and Martian orbits measured with respect to the vernal equinox. Finally, if Ξ_E and Ξ_M are the longitudes of the planets at the epoch, then, correspondingly, at a time T years from epoch their mean anomalies, M_E and M_M are given by

$$M_E = 2\pi T + \Xi_E - \Pi_E \tag{3.1.1}$$

$$M_M = (2\pi T/P_M) + \Xi_M - \Pi_M \tag{3.1.2}$$

where P_M, the period of Mars in years, is given by

$$P_M = (a_M/a_E)^{3/2} \tag{3.1.3}$$

From the mean anomalies, we may compute the eccentric anomalies E_E and E_M by means of the Fourier-Bessel expansions

$$E_E = M_E + 2\sum_{n=1}^{\infty} (1/n)J_n(n\epsilon_E) \sin nM_E \tag{3.1.4}$$

$$E_M = M_M + 2\sum_{n=1}^{\infty} (1/n)J_n(n\epsilon_M) \sin nM_M \tag{3.1.5}$$

where J_n is a Bessel function of the first kind of order n. The position vectors $\boldsymbol{r}_E$ and $\boldsymbol{r}_M$ at time T may then be determined from

$$\begin{aligned}\boldsymbol{r}_E = {} & [a_E \cos \Pi_E(\cos E_E - \epsilon_E) - \\ & \sqrt{a_E l_E} \sin \Pi_E \sin E_E]\boldsymbol{i}_x + \\ & [a_E \sin \Pi_E (\cos E_E - \epsilon_E) + \\ & \sqrt{a_E l_E} \cos \Pi_E \sin E_E]\boldsymbol{i}_y\end{aligned} \tag{3.1.6}$$

$$\boldsymbol{r}_M = a_M(\cos E_M - \epsilon_M)\boldsymbol{i}_\xi + \sqrt{a_M l_M} \sin E_M \boldsymbol{i}_\eta \tag{3.1.7}$$

In order to obtain the components of the Martian position vector $\boldsymbol{r}_M$ in the ecliptic coordinate system, one may simply pre-multiply the vector $\boldsymbol{r}_M$, regarded as a column vector, by the matrix

$$\mathfrak{M} = \begin{pmatrix} l_1 & l_2 & l_3 \\ m_1 & m_2 & m_3 \\ n_1 & n_2 & n_3 \end{pmatrix} \tag{3.1.8}$$

where $l_1 = \cos \Omega \cos \omega - \sin \Omega \sin \omega \cos i$
$l_2 = -\cos \Omega \sin \omega - \sin \Omega \cos \omega \cos i$

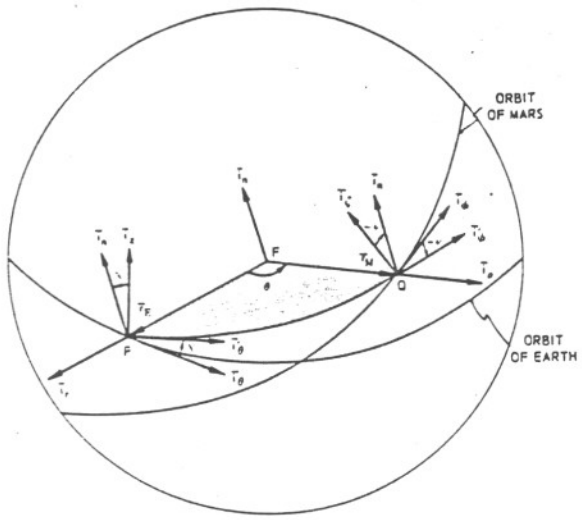

χ = ANGLE OF INCLINATION OF TRAJECTORY PLANE TO PLANE OF THE ECLIPTIC
ν = ANGLE OF INCLINATION OF TRAJECTORY PLANE TO PLANE OF THE MARTIAN ORBIT

FIG. 3-2. Local polar coordinate systems of Earth, Mars, and spaceship orbits.

$$
\begin{aligned}
l_3 &= \sin\Omega \sin i \\
m_1 &= \sin\Omega \cos\omega + \cos\Omega \sin\omega \cos i \\
m_2 &= -\sin\Omega \sin\omega + \cos\Omega \cos\omega \cos i \\
m_3 &= -\cos\Omega \sin i \\
n_1 &= \sin\omega \sin i \\
n_2 &= \cos\omega \sin i \\
n_3 &= \cos i
\end{aligned}
$$

Consider now the problem of connecting a point P on the Earth's orbit and a point Q on the Martian orbit by an ellipse whose focus F is sun-centered, as illustrated in Fig. 3-2. Let $\boldsymbol{r}_E$ and $\boldsymbol{r}_M$ represent the vector positions of P and Q. Then the cosine of the angle θ between $\boldsymbol{r}_E$ and $\boldsymbol{r}_M$ is obtained from

$$\cos\theta = (\boldsymbol{r}_E \cdot \boldsymbol{r}_M)/r_E r_M \tag{3.1.9}$$

Since θ is measured in the direction of motion of the planets, the sine of the angle, with appropriate consideration for sign, is given by

$$\sin\theta = \operatorname{sgn}(\boldsymbol{r}_E \times \boldsymbol{r}_M \cdot \boldsymbol{i}_z)\sqrt{1 - \cos^2\theta} \tag{3.1.10}$$

The unit vector $\boldsymbol{i}_n$ normal to the plane of the ellipse and having a positive component in the $\boldsymbol{i}_z$ direction may then be obtained from

$$\boldsymbol{i}_n = (\boldsymbol{r}_E \times \boldsymbol{r}_M)/r_E r_M \sin\theta \tag{3.1.11}$$

When computing the vector velocities of the Earth and spaceship at the point P, it will be convenient to use a local polar coordinate system centered at P, with unit vector $\boldsymbol{i}_r$ in the positive direction of $\boldsymbol{r}_E$ and with $\boldsymbol{i}_\theta$ chosen in the plane of the ecliptic and such that $\boldsymbol{i}_r$, $\boldsymbol{i}_\theta$ and $\boldsymbol{i}_z$ form the right-handed triad shown in Fig. 3-2. The plane of the ellipse is inclined at an angle χ to the ecliptic, with the angle positive in the direction of a right-handed rotation about $\boldsymbol{i}_r$. Hence,

$$\cos\chi = \boldsymbol{i}_n \cdot \boldsymbol{i}_z \tag{3.1.12}$$

One may readily see that χ is positive if, simultaneously, θ is less than 180° and the point Q is above the ecliptic or, alternately, θ is greater than 180° and Q is below the ecliptic; otherwise, χ is negative. These facts may be summarized conveniently by means of the equation

$$\sin\chi = \operatorname{sgn}(\boldsymbol{r}_M \cdot \boldsymbol{i}_z \sin\theta)\sqrt{1 - \cos^2\chi} \tag{3.1.13}$$

Similarly, at the point Q we introduce a set of unit vectors $\boldsymbol{i}_\rho$ and $\boldsymbol{i}_\phi$, as shown in Fig. 3-2. The angle ν is the inclination angle of the trajectory plane with respect to the plane of the Martian orbit and is positive in the direction of a right-handed rotation about $\boldsymbol{i}_\rho$. Therefore,

$$\cos\nu = \boldsymbol{i}_n \cdot \boldsymbol{i}_\rho \tag{3.1.14}$$

Again one sees that ν is negative if, simultaneously, θ is less than 180° and the point P is above the Martian plane or, alternately, θ is greater than 180° and P is below the Martian plane; otherwise. ν is positive. Hence,

$$\sin\nu = \operatorname{sgn}(-\boldsymbol{r}_E \cdot \boldsymbol{i}_r \sin\theta)\sqrt{1 - \cos^2\nu} \tag{3.1.15}$$

We shall close this preliminary section with the derivation of a criterion for determining the sign of the radial component of the vector velocity of the spaceship at the points P and Q. For this purpose, let us define the vector $\boldsymbol{i}_F$ as a unit vector from the center of force F and in the direction of the vacant focus of the ellipse. Since $\boldsymbol{i}_F$ lies in the plane containing both $\boldsymbol{r}_E$ and $\boldsymbol{r}_M$, it may be expressed as a linear combination of these two vectors—i.e.,

$$\boldsymbol{i}_F = F_E \boldsymbol{r}_E + F_M \boldsymbol{r}_M \tag{3.1.16}$$

By taking the scalar product of $\boldsymbol{i}_F$ with $\boldsymbol{r}_E$ and $\boldsymbol{r}_M$ in turn, we have

$$\boldsymbol{i}_F \cdot \boldsymbol{r}_E = F_E r_E^2 + F_M r_E r_M \cos\theta$$

$$\boldsymbol{i}_F \cdot \boldsymbol{r}_M = F_E r_E r_M \cos\theta + F_M r_M^2$$

But if θ_0 is the angle between $\boldsymbol{r}_E$ and $\boldsymbol{i}_F$, and l and ϵ are, respectively, the semi-latus rectum and eccentricity of the ellipse, then, using the polar-coordinate equation for an ellipse, given by Eq. (1.5.1),

$$\boldsymbol{i}_F \cdot \boldsymbol{r}_E = r_E \cos\theta_0 = (r_E - l)/\epsilon$$

$$\boldsymbol{i}_F \cdot \boldsymbol{r}_M = r_M \cos(\theta_0 - \theta) = (r_M - l)/\epsilon$$

Hence, solving for F_E and F_M, we obtain

$$F_E = (1/\epsilon r_E \sin^2\theta)\{[1 - (l/r_E)] - [1 - (l/r_M)]\cos\theta\} \tag{3.1.17}$$

$$F_M = (1/\epsilon r_M \sin^2\theta)\{[1 - (l/r_M)] - [1 - (l/r_E)]\cos\theta\} \tag{3.1.18}$$

At the point P, the radial component of the vector velocity of the spaceship and the component of the vector $\boldsymbol{r}_E \times \boldsymbol{r}_F$ in the $\boldsymbol{i}_n$ direction have identical signs. Therefore, it follows from Eqs. (3.1.16) and (3.1.11) that the spaceship will be moving away from or toward the sun according to whether the sign of $F_M \sin\theta$ is respectively positive or negative. Similarly, at the point Q, the corresponding criterion is the sign of $-F_E \sin\theta$.

(3.2) *Procedure for Calculating Round-Trip Trajectories*

Essentially the same technique described in Section (2.4) for determining round-trip reconnaissance trajectories in the simplified model of the solar system may be used in the three-dimensional version. One fundamental difference occurs in the method of estimating the point on the Martian orbit where planetary contact can occur and, subsequently, the point at which the spaceship will return to the Earth. With circular symmetry no longer a characteristic of the model, we are not free to choose arbitrarily the heliocentric angle θ. However, if we postulate a departure time, T_H, measured in years from the epoch, we may, instead, estimate the time T_{EM} required for the voyage from Earth to Mars and the time T_{ME} for return. The net effect is, of course, the same, in that the angles θ_D and θ_R are direct functions of these times. As an aid in the estimation of the times T_D, T_{EM}, and T_{ME}, the results obtained for the two-dimensional model can be used to advantage.

The two methods also differ in the manner of determining the semi-major axis of the spaceship orbit. We have no three-dimensional analog of Eq. (2.1.7); instead, since the times of flight are fixed by our initial estimate, the time-of-flight equation (2.4.1) must serve as the means for calculating a_D and a_R.

If, in addition to the departure time, T_D, we specify the relative departure velocity magnitude, V_{RE}, it will be necessary to repeat the calculation of a_D while systematically varying the time T_{EM} in order to obtain a trajectory that satisfies this additional requirement. Under any circumstances, this procedure will be mandatory for calculating the return-trip trajectory since the vehicle must leave Mars with the same relative velocity magnitude, V_{RM}, with which it arrived.

Before detailing the step-by-step process, let us turn our attention briefly to the problem of solving the time-of-flight formula for the semi-major axis a. Curves of the time of flight, T, as a function of a were computed from Eq. (2.4.1) and are plotted in Fig. 3-3 for several values of θ. If the angle θ is less than 360° ($N = 0$), Eq. (2.4.1) defines a as a single-valued function of T. Therefore, if a trajectory connecting the points P and Q is possible for a given value of T, it is unique. On the other hand, if θ is greater than 360°, a is a doubled-valued function of T. Thus, corresponding to each value of T that is sufficiently large to ensure a solution, two different trajectories are obtained.

For the case in which $N = 0$, the procedure for obtaining a is straightforward. We first compute the time of flight T_m for the minimum-energy path, for which $a = a_m$ or, equivalently, $\alpha = \pi$, from the formula

$$T_m = (P_m/2)\{1 - [\text{sgn}\,(\sin\theta)/\pi](\beta_m - \sin\beta_m)\} \tag{3.2.1}$$

Then by comparing the given value of T with T_m, we find that the upper or lower sign is appropriate in Eq. (2.4.1) according to whether T is, respectively, less than or greater than T_m. However, if T is less than

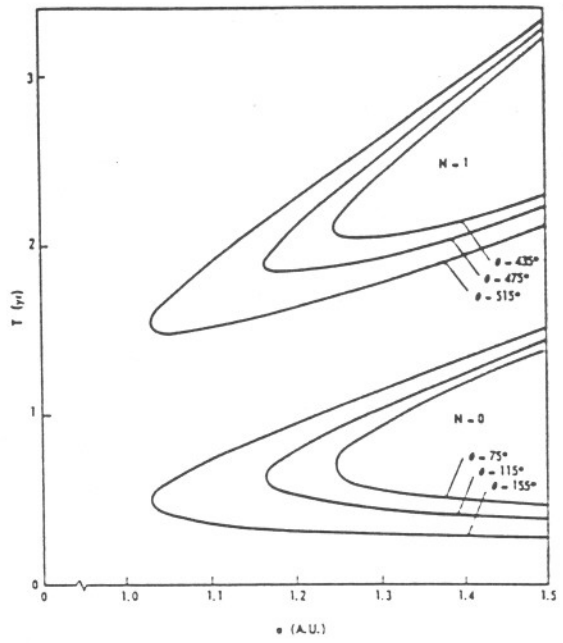

FIG. 3-3. Time of flight from Earth to Mars vs. semi-major axis of transfer ellipse for various values of the polar angle θ.

the time T_p required to travel the parabolic path from P to Q, where

$$T_p = (1/3)\sqrt{2/\mu_s}\,[s^{3/2} - \text{sgn}\,(\sin\theta)(s - c)^{3/2}] \tag{3.2.2}$$

then no solution for elliptical trajectories is possible. With the feasibility of the elliptical orbit confirmed and the appropriate sign determined for Eq. (2.4.1), a simple iteration will produce the unique root.

The situation is somewhat more complex when N is not zero. If a relevant two-dimensional solution to the trajectory problem is available, it can be used to advantage in selecting the proper branch of the curve a as a function of T. In the absence of any such information, one can always proceed with the computation, using both roots, and reject whichever proves unsatisfactory.

Returning now to the main problem, we shall outline a procedure for calculating a nonstop trajectory for a voyage from Earth to Mars and return, to begin on a specific date with a prescribed relative departure velocity magnitude.

(1) A departure time, T_D, is specified that is measured in years from the epoch.

(2) The mean anomaly of the Earth at the point of departure, $M_E(T_D)$, is computed from Eq. (3.1.1). Then, from Eq. (3.1.4), the corresponding eccentric anomaly of the Earth, $E_E(T_D)$, is obtained. Finally, the vector position of the Earth at the time of departure, $r_E(T_D)$, is computed from Eq. (3.1.6).

(3) The vector velocity of the Earth at time T_D is obtained from

$$V_E(T_D) = \text{sgn}\,[\sin E_E(T_D)] \times \sqrt{\mu_s\{[(2r_E - l_E)/r_E^2] - (1/a_E)\}}\,i_r + (\sqrt{\mu_s l_E}/r_E)i_\theta \tag{3.2.3}$$

(4) An estimate of the time T_{EM} in years required for the voyage from Earth to Mars is made and the mean anomaly of Mars, $M_M(T_D + T_{EM})$, for the point at which contact with the spaceship will occur is computed from Eq. (3.1.2). The corresponding eccentric anomaly, $E_M(T_D + T_{EM})$, and vector position, $\mathbf{r}_M(T_D + T_{EM})$, are then obtained from Eqs. (3.1.5) and (3.1.7).

(5) The heliocentric angle θ_D, through which the spaceship moves on the departure orbit, is calculated using Eqs. (3.1.9) and (3.1.10), from which the linear distance c, measured from the point of departure P to the point of arrival Q at Mars, is obtained from

$$c^2 = r_E^2 + r_M^2 - 2r_E r_M \cos\theta_D \tag{3.2.4}$$

(6) From the time-of-flight equation (2.4.1), with $T = T_{EM}$, the semi-major axis a_D of the departure orbit is obtained. Then the semi-latus rectum l_D is computed from Eq. (1.5.9), with the choice of upper or lower sign made to correspond with the sign used in Eq. (2.4.1) to produce the root a_D.

(7) The vector $\mathbf{i}_n$ normal to the plane of the departure trajectory is computed from Eq. (3.1.11) and the result used in Eqs. (3.1.12) and (3.1.13) to obtain the inclination angle χ.

(8) The velocity vector V_{PE} of the spaceship at the point of departure is computed from

$$V_{PE} = \text{sgn}\,(F_M \sin\theta_D) \times \sqrt{\mu_s\{[(2r_E - l_D)/r_E^2] - (1/a_D)\}}\,\mathbf{i}_r + (\sqrt{\mu_s l_D}/r_E)(\cos\chi\mathbf{i}_\theta + \sin\chi\mathbf{i}_z) \tag{3.2.5}$$

where F_M is defined in Eq. (3.1.18).

(9) The vector velocity V_{RE} of the spaceship relative to the Earth at the point of departure P may then be computed as the vector difference

$$V_{RE} = V_{PE} - V_E(T_D) \tag{3.2.6}$$

(10) The magnitude of the relative velocity V_{RE} may now be compared with the prescribed value. If the two differ by more than a tolerable amount, a new estimate for T_{EM} must be made and steps (4) through (9) repeated.

(11) When an Earth-to-Mars orbit has been found that satisfies the initial departure conditions, we may then determine the relative velocity of the spaceship at Q, the point of contact with Mars. For this purpose, the vector velocity of Mars at time $T_D + T_{EM}$ is computed from

$$V_M(T_D + T_{EM}) = \text{sgn}\,[\sin E_M(T_D + T_{EM})] \times \sqrt{\mu_s\{[(2r_M - l_M)/r_M^2] - (1/a_M)\}}\,\mathbf{i}_\rho + (\sqrt{\mu_s l_M}/r_M)\mathbf{i}_\phi \tag{3.2.7}$$

and the vector velocity of the spaceship at the point Q from

$$V_{QM} = \text{sgn}\,(-F_E \sin\theta_D) \times \sqrt{\mu_s\{[(2r_M - l_D)/r_M^2] - (1/a_D)\}}\,\mathbf{i}_\rho + (\sqrt{\mu_s l_D}/r_M)(\cos\nu\mathbf{i}_\phi + \sin\nu\mathbf{i}_\zeta) \tag{3.2.8}$$

where F_E is defined in Eq. (3.1.17) and the inclination angle ν is obtained using Eqs. (3.1.14) and (3.1.15). Finally, the relative velocity V_{RM} is computed as the vector difference

$$V_{RM} = V_{QM} - V_M(T_D + T_{EM}) \tag{3.2.9}$$

(12) To obtain a return trajectory, the procedure is precisely the same. The spaceship departs from Mars at time $T_D + T_{EM}$ and arrives at Earth T_{ME} years later. As before, the time for the trip from Mars to Earth is a result of the iteration process used for determining a trajectory whose relative velocity magnitude V_{RM} at Mars is prescribed.

(13) As a final step, we must determine the orientation of the spaceship with respect to Mars that must be effected during the period of contact in order to accomplish the transfer from the departure orbit to the return orbit. Let V_{RMD} and V_{RMR} be, respectively, the relative velocities with respect to Mars of the vehicle on the departure orbit and the return orbit. The turn angle 2δ may be computed from

$$\sin 2\delta = \frac{|V_{RMR} \times V_{RMD}|}{V_{RM}^2} \tag{3.2.10}$$

and the passing distance D from Eq. (2.4.3).

If the vector product in Eq. (3.2.10) has a positive component in the ζ direction, we shall say that the spaceship passes ahead of Mars; otherwise, the ship passes behind the planet. Furthermore, this vector product defines the orientation of the plane of relative approach to Mars.

(3.3) *Comparison of Results With the Simplified Model*

The computational procedure for determining three-dimensional round-trip trajectories has been programed for a digital computer. The input to the program consists of a departure time T_D and a departure velocity V_{RE}, together with estimates of the times required for the trips to and from Mars.

Several of the two-dimensional trajectories found in Section (2) were recalculated in the three-dimensional model. The same departure velocity of 0.13 times the Earth's orbital speed, or 12,709 ft. per sec., was used. The time of departure T_D was selected so that the difference of the mean longitudes of the planets would be the same as the heliocentric angular difference A_{EM} between Earth and Mars found in the two-dimensional solution. The time-of-flight estimates were likewise taken directly from the results in the simplified model.

For comparison purposes, the corresponding trajectories are represented schematically in Figs. 3-4 through 3-9. In each case, the circles shown are sun-centered, with radii equal to the mean distances of the Earth and Mars. The major axes of the true elliptical orbits of the planets are shown as broken lines, with the perihelions and aphelions appropriately marked P_E, A_E, and P_M, A_M. The line of nodes is also shown as a broken line, with the ascending and descending nodes labeled AN and DN. The positions of the planets at the times of departure, arrival at Mars, and return to the Earth are denoted by the letters E and M with

respective subscripts D, A, and R. The point of departure from the Earth E_D is approximately the same for two models; however, the points of arrival at Mars and return to Earth are different. The primed symbols correspond to the three-dimensional model, while the unprimed symbols correspond to the two-dimensional model. The major axes of the departure and return orbits for both cases are shown as solid lines, with the perihelion and aphelion points labeled and the positions of the vacant foci marked.

Together with the diagrams are shown some of the data for the three-dimensional trajectories. These data may be compared with Table 1 of Section (2). As a result of this comparison, certain general conclusions may be drawn, which are discussed below.

The most striking difference between the two models is seen for those trajectories in which the point of departure from the Earth and the point of arrival at the planet are nearly 180° apart. For the case of co-planar planetary orbits we have seen that this configuration of the planets gives rise to the absolute minimum-energy transfer ellipse. In the three-dimensional model, even though the angle between the two planes is less than 2°, the situation is considerably altered. If the diametrical position of the points of departure and arrival lie on the line of nodes, the orbital plane of the spaceship may be chosen arbitrarily. On the other hand, since this plane must always contain the three points determined by the positions of Earth, sun, and Mars, a large angle of inclination to the ecliptic can result when these three points are not distributed on the line of nodes. In particular, when the diametrical position of the planets is at right angles to the line of intersection of the orbital planes of the planets, the trajectory plane will be at right angles to the plane of the ecliptic.

This point is rather dramatically illustrated when trajectories No. 1 and No. 6 are contrasted. In many respects the two seem alike. For each, the spaceship leaves at roughly the same time, contacts Mars at essentially the same point in space after some six months, and each returns to Earth at approximately the same position. However, we note that for the return orbit the points of arrival at Mars and return to Earth are 184.76° apart for trajectory No. 1 and 182.75° apart for trajectory No. 6. The inclination angles of the return orbits are, respectively, 4.671° and 14.481°. We further note, in the latter case, that a 44° rotation of the relative velocity vector at Mars must be effected in order to transfer from the departure orbit to the return orbit. The gravitational field of Mars is inadequate to accomplish this transfer, as seen from the fact that a mathematical solution is obtained only by permitting the spaceship to pass more than 1,200 miles beneath the Martian surface.

Still another difference between the two models is apparent in the manner of approaching Mars. In the two-dimensional model, all motion takes place in a single plane. Even in the three-dimensional model, except for the singular situation noted, the inclination

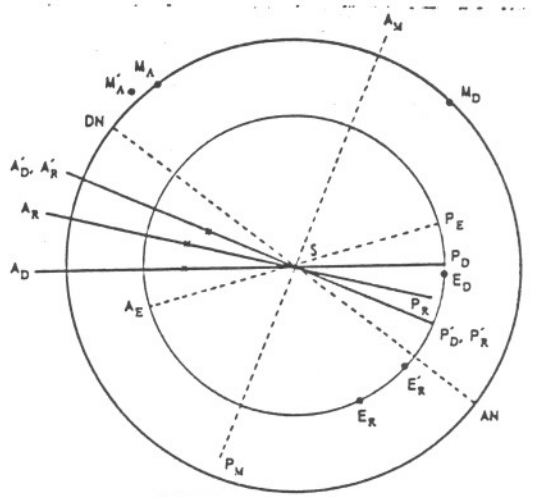

DEPARTURE TIME: DECEMBER 13, 1964

DEPARTURE ORBIT:

θ_D = 135.79°
$\bar{V}_{RED}$ = $6943\bar{i}_r + 10591\bar{i}_\theta + 1065\bar{i}_z$
$\bar{V}_{RMD}$ = $17016\bar{i}_\rho - 7597\bar{i}_\phi + 1684\bar{i}_\zeta$
V_{RED} = 12709 ft/sec
V_{RMD} = 18711 ft/sec
$r_E(T_D)$ = 0.9843 A.U.
$r_M(T_D + T_{EM})$ = 1.5800 A.U.
T_D = 6.951 years
T_{EM} = 0.5262 years
a_D = 1.3091 A.U.
ϵ_D = 0.2543
x_D = 0.555°
ν_D = 1.409°

RETURN ORBIT:

θ_R = 544.76°
$\bar{V}_{RER}$ = $-7063\bar{i}_r + 10128\bar{i}_\theta + 8882\bar{i}_z$
$\bar{V}_{RMR}$ = $16721\bar{i}_\rho - 7679\bar{i}_\phi - 3291\bar{i}_\zeta$
V_{RER} = 15210 ft/sec
T_{ME} = 2.3669 years
a_R = 1.3076 A.U.
ϵ_R = 0.2532
x_R = 4.671°
ν_R = −2.840°

PLANETARY CONTACT:

2δ = 15.619°
d = 3110 miles

THE VEHICLE PASSES AHEAD OF MARS IN A PLANE INCLINED 87.266° TO THE MARTIAN ORBIT.

FIG. 3-4. Trajectory No. 1.

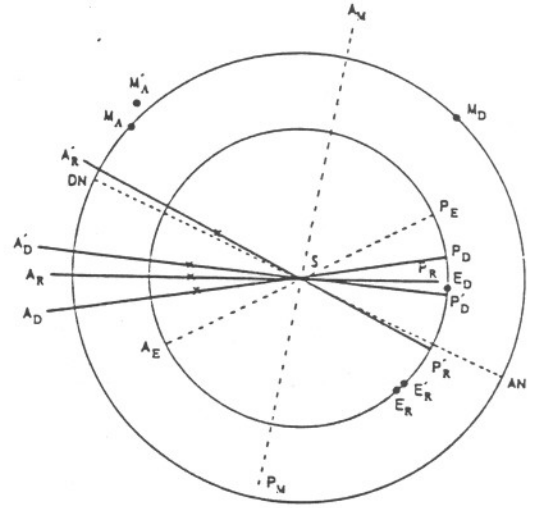

DEPARTURE TIME: DECEMBER 4, 1964

DEPARTURE ORBIT:

θ_D = 134.87°
$\bar{V}_{RED}$ = $1865\bar{i}_r + 12428\bar{i}_\theta + 1889\bar{i}_z$
$\bar{V}_{RMD}$ = $22667\bar{i}_\rho - 6338\bar{i}_\phi + 1236\bar{i}_\zeta$
V_{RED} = 12709 ft/sec
V_{RMD} = 23569 ft/sec
$r_E(T_D)$ = 0.9854 A.U.
$r_M(T_D + T_{EM})$ = 1.6023 A.U.
T_D = 6.927 years
T_{EM} = 0.4943 years
a_D = 1.3785 A.U.
ϵ_D = 0.2853
x_D = 0.970°
ν_D = 1.031°

RETURN ORBIT:

θ_R = 542.75°
$\bar{V}_{RER}$ = $-7462\bar{i}_r + 7293\bar{i}_\theta + 27266\bar{i}_z$
$\bar{V}_{RMR}$ = $15873\bar{i}_\rho - 8971\bar{i}_\phi - 14934\bar{i}_\zeta$
V_{RER} = 29194 ft/sec
T_{ME} = 2.3902 years
a_R = 1.3185 A.U.
ϵ_R = 0.2583
x_R = 14.481°
ν_R = −12.747°

PLANETARY CONTACT:

2δ = 44.204°
d = −1252 miles

THE VEHICLE PASSES AHEAD OF MARS IN A PLANE INCLINED 73.862° TO THE MARTIAN ORBIT.

FIG. 3-5. Trajectory No. 6.

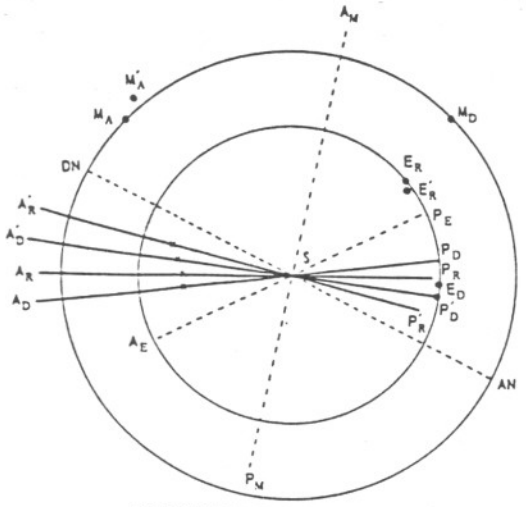

DEPARTURE TIME: DECEMBER 4, 1964

DEPARTURE ORBIT:

$\theta_D = 134.87°$
$\bar{V}_{RED} = 1865\bar{i}_r + 12428\bar{i}_\theta + 1889\bar{i}_z$
$\bar{V}_{RMD} = 22667\bar{i}_\rho - 6338\bar{i}_\phi - 1236\bar{i}_\zeta$
$V_{RED} = 12709$ ft/sec
$V_{RMD} = 23569$ ft/sec
$r_E(T_D) = 0.9854$ A.U.
$r_M(T_D + T_{EM}) = 1.6023$ A.U.
$T_D = 6.927$ years
$T_{EM} = 0.4943$ years
$a_D = 1.3785$ A.U.
$\epsilon_D = 0.2853$
$\chi_D = 0.970°$
$\nu_D = 1.031°$

RETURN ORBIT:

$\theta_R = 624.95°$
$\bar{V}_{RER} = 21947\bar{i}_r + 8577\bar{i}_\theta + 1301\bar{i}_z$
$\bar{V}_{RMR} = 21805\bar{i}_\rho - 8739\bar{i}_\phi + 1916\bar{i}_\zeta$
$V_{RER} = 23599$ ft/sec
$T_{ME} = 2.6128$ years
$a_R = 1.3123$ A.U.
$\epsilon_R = 0.3176$
$\chi_R = 0.690°$
$\nu_R = 1.656°$

PLANETARY CONTACT:

$2\delta = 6.420°$
$d = 6611$ miles

THE VEHICLE PASSES AHEAD OF MARS IN A PLANE INCLINED 16.598° TO THE MARTIAN ORBIT.

FIG. 3-6. Trajectory No. 7.

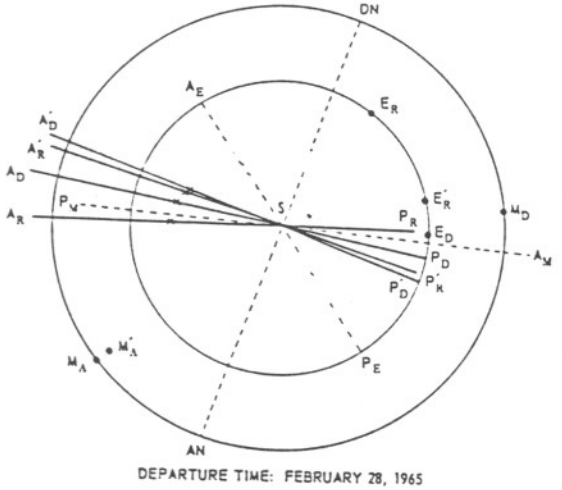

DEPARTURE TIME: FEBRUARY 28, 1965

DEPARTURE ORBIT:

$\theta_D = 219.91°$
$\bar{V}_{RED} = 6185\bar{i}_r + 10749\bar{i}_\theta + 2780\bar{i}_z$
$\bar{V}_{RMD} = -24593\bar{i}_\rho - 8368\bar{i}_\phi - 3628\bar{i}_\zeta$
$V_{RED} = 12709$ ft/sec
$V_{RMD} = 26230$ ft/sec
$r_E(T_D) = 0.9906$ A.U.
$r_M(T_D + T_{EM}) = 1.4148$ A.U.
$T_D = 7.160$ years
$T_{EM} = 1.0744$ years
$a_D = 1.3168$ A.U.
$\epsilon_D = 0.2565$
$\chi_D = 1.455°$
$\nu_D = -2.713°$

RETURN ORBIT:

$\theta_R = 510.00°$
$\bar{V}_{RER} = 9054\bar{i}_r + 10232\bar{i}_\theta - 3543\bar{i}_z$
$\bar{V}_{RMR} = -24360\bar{i}_\rho - 8730\bar{i}_\phi - 4280\bar{i}_\zeta$
$V_{RER} = 14114$ ft/sec
$T_{ME} = 1.9527$ years
$a_R = 1.3062$ A.U.
$\epsilon_R = 0.2574$
$\chi_R = 1.868°$
$\nu_R = -3.215°$

PLANETARY CONTACT:

$2\delta = 1.706°$
$d = 25519$ miles

THE VEHICLE PASSES BEHIND MARS IN A PLANE INCLINED -33.518° TO THE MARTIAN ORBIT.

FIG. 3-7. Trajectory No. 9.

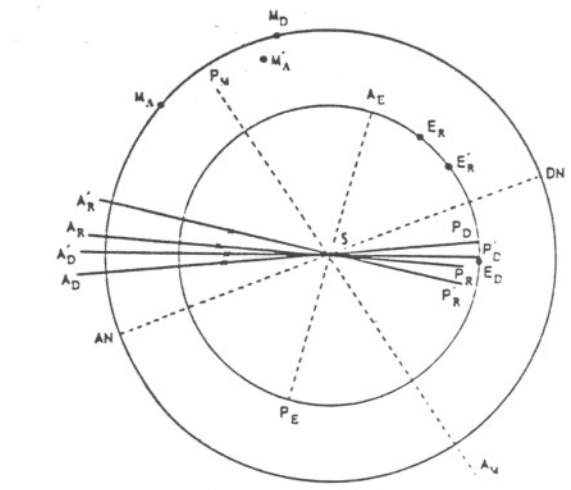

DEPARTURE TIME: APRIL 27, 1960

DEPARTURE ORBIT:

$\theta_D = 470.43°$
$\bar{V}_{RED} = -1796\bar{i}_r - 12016\bar{i}_\theta - 3729\bar{i}_z$
$\bar{V}_{RMD} = 22047\bar{i}_\rho - 7409\bar{i}_\phi + 613\bar{i}_\zeta$
$V_{RED} = 12709$ ft. sec
$V_{RMD} = 23266$ ft/sec
$r_E(T_D) = 1.0066$ A.U.
$r_M(T_D + T_{EM}) = 1.3828$ A.U.
$T_D = 2.319$ years
$T_{EM} = 1.9259$ years
$a_D = 1.3523$ A.U.
$\epsilon_D = 0.2556$
$\chi_D = -1.957°$
$\nu_D = 0.442°$

RETURN ORBIT:

$\theta_R = 287.34°$
$\bar{V}_{RER} = 17295\bar{i}_r + 8577\bar{i}_\theta - 3519\bar{i}_z$
$\bar{V}_{RMR} = 21040\bar{i}_\rho - 9871\bar{i}_\phi - 1092\bar{i}_\zeta$
$V_{RER} = 19623$ ft/sec
$T_{ME} = 1.1814$ years
$a_R = 1.2755$ A.U.
$\epsilon_R = 0.2634$
$\chi_R = 1.921°$
$\nu_R = 0.812°$

PLANETARY CONTACT:

$2\delta = 7.785°$
$d = 5179$ miles

THE VEHICLE PASSES AHEAD OF MARS IN A PLANE INCLINED 32.082° TO THE MARTIAN ORBIT.

FIG. 3-8. Trajectory No. 11.

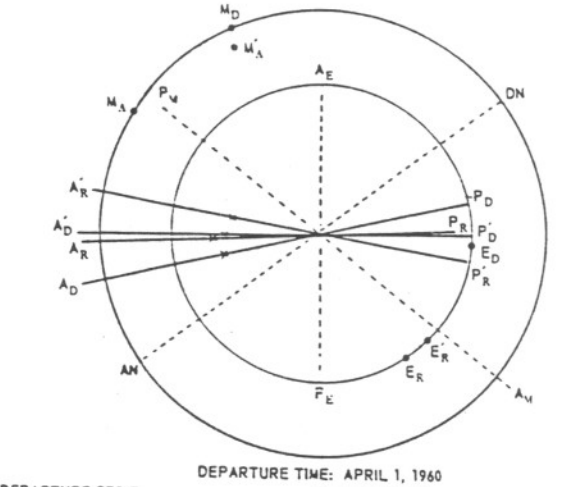

DEPARTURE TIME: APRIL 1, 1960

DEPARTURE ORBIT:

$\theta_D = 478.71°$
$\bar{V}_{RED} = -3557\bar{i}_r - 11535\bar{i}_\theta - 3976\bar{i}_z$
$\bar{V}_{RMD} = 23375\bar{i}_\rho - 7774\bar{i}_\phi + 1771\bar{i}_\zeta$
$V_{RED} = 12709$ ft. sec
$V_{RMD} = 24698$ ft. sec
$r_E(T_D) = 0.9995$ A.U.
$r_M(T_D + T_{EM}) = 1.3929$ A.U.
$T_D = 2.250$ years
$T_{EM} = 1.9235$ years
$a_D = 1.3364$ A.U.
$\epsilon_D = 0.2527$
$\chi_D = -2.883°$
$\nu_D = 1.293°$

RETURN ORBIT:

$\theta_R = 201.61°$
$\bar{V}_{RER} = -13801\bar{i}_r - 8817\bar{i}_\theta + 9353\bar{i}_z$
$\bar{V}_{RMR} = 21690\bar{i}_\rho - 9817\bar{i}_\phi - 6567\bar{i}_\zeta$
$V_{RER} = 18859$ ft/sec
$T_{ME} = 0.9675$ years
$a_R = 1.2755$ A.U.
$\epsilon_R = 0.2512$
$\chi_R = 4.965°$
$\nu_R = 4.909°$

PLANETARY CONTACT:

$2\delta = 12.736°$
$d = 1666$ miles

THE VEHICLE PASSES AHEAD OF MARS IN A PLANE INCLINED 63.873° TO THE MARTIAN ORBIT.

FIG. 3-9. Trajectory No. 13.

angles of the planes of motion of the spaceship are small. However. as viewed from the surface of Mars, the angular orientation of the plane of approach is certainly not small. Thus in the vicinity of Mars, the true relative motion of the spaceship and planet is not at all adequately approximated by the two-dimensional model.

A third point of contrast has to do not so much with the three-dimensional nature of the solar system as with the ellipticity of the planetary orbits. In the elementary model, the planets were assumed to move in concentric circles about the sun whose radii were taken as the corresponding mean distances. The approximation is relatively good for the Earth, whose eccentricity is only about 0.0167. However, for Mars with an eccentricity in excess of 0.0937, the difference between the closest and farthest distance from the sun is almost 3/10 of an astronomical unit.

The effects of the ellipticity of the Martian orbit were very apparent when the three-dimensional solution for trajectory No. 1 was attempted. Since the difference of the mean longitudes of the two planets Earth and Mars is the same every 2.135 years, it would seem at first that departure dates that differ by this amount should produce essentially the same solutions. However, primarily because of the variation in the distance from Mars to the sun, it was impossible to obtain a departure orbit for trajectory No. 1 with a departure velocity of 0.13 times the Earth's orbital velocity before 1964. For earlier dates, the point of contact with Mars occurred too near the aphelion of the planet.

One final comment seems appropriate concerning the relative merits of the several trajectories considered. Although the departure velocities were all the same, the velocities with which the spaceship returns to Earth are seen to vary from 14,000 to well over 20,000 ft. per sec. These differences are of fundamental importance to the problem of re-entry of the vehicle into the Earth's atmosphere.

(3.4) *A Class of Round-Trip Trajectories*

The particular solutions to the round-trip problem discussed in the previous section serve to illustrate some of the various types of possible reconnaissance trajectories. However, one should not infer that such solutions are isolated events. On the contrary, during appropriate seasons of the year, round-trip trajectory solutions exist as a continuous function of the departure time. It is of interest to determine how certain characteristics of these solutions vary with the time and velocity of departure.

For this purpose, the particular class of trajectories, of which trajectory No. 7 is a representative member, was examined in full detail. Three departure velocities were selected—namely, 12,200, 13,000 and 13,800 ft. per sec. Then solutions corresponding to these velocities were obtained at various instants of time, both earlier and later than December 4, 1964, which is the departure time for trajectory No. 7. To obtain a continuous pattern of solutions, regular intervals of time

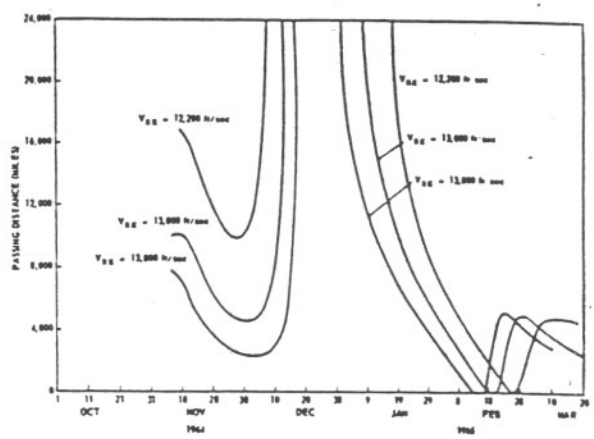

FIG. 3-10. Passing distance at Mars vs. departure date for various values of departure velocity.

were selected and the time-of-flight estimates needed for the digital computer program were made sequentially, based on the time requirements of each previously obtained solution. In this way, we were assured of producing only the trajectory solutions belonging to one particular class. The interval of departure times during which solutions were obtained using this procedure extends from early in November, 1964, until late in March, 1965. Immediately prior to November, 1964, and just after March, 1965, the configuration of the planets is unfavorable for a reconnaissance mission with the stated velocity specifications.

In the accompanying figures, a few of the important elements of these solutions are plotted as a function of the departure time. The passing distance at the point of closest approach to the surface of Mars is shown in Fig. 3-10. During the first week in November, 1964, the point of departure from Earth and the point of arrival at Mars are nearly 180° apart. No solutions were obtained in this period because of the excessive velocity requirements out of the plane of the ecliptic. As time increases, the departure angle θ_D decreases and round-trip solutions are possible. From late in November to the early part of December. each of the constant-departure-velocity curves attains a minimum. Within ten days following the minimum, the required passing distance increases to such an extent that planetary contact becomes impossible.

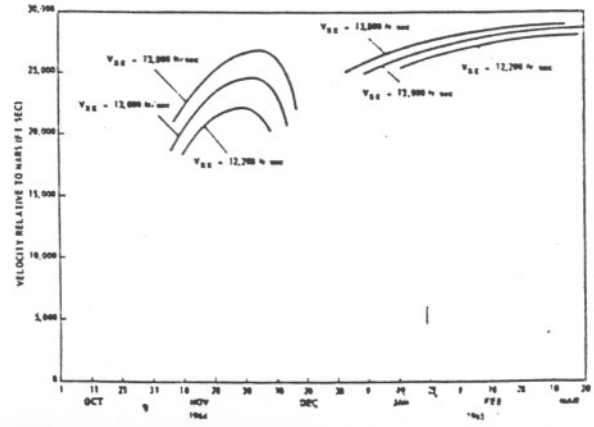

FIG. 3-11. Velocity relative to Mars vs. departure date for various values of departure velocity.

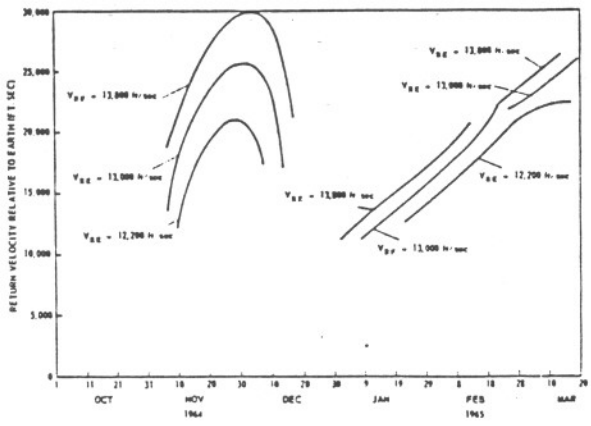

FIG. 3-12. Return velocity relative to Earth vs. departure date for various values of departure velocity.

Early in January, 1965, solutions are again obtained; the required passing distance decreases steadily until sometime in the middle of February, when mathematical solutions are possible only by permitting the point of closest approach to fall below the Martian surface. During this period of time in February, the point of arrival at Mars and the point of return to Earth are nearly 180° apart. Later in February and early in March, the return angle θ_R increases and physically realizable solutions are again possible.

In Fig. 3-11, the velocity of the spaceship relative to Mars is plotted as a function of departure time. Similarly, the velocity relative to the Earth with which the spaceship returns to Earth is shown in Fig. 3-12. For the particular choice of departure velocities, the velocities relative to Mars vary from 18,000 to 27,000 ft. per sec. during 1964 and from 25 000 to 29,000 ft. per sec. during 1965. The variations in the return velocity are much greater and, indeed, we observe the curious fact that the spaceship can return to Earth with a velocity smaller than the one with which it left.

In 1964, all solutions require the spaceship to move through a heliocentric angular distance of less than 180° for the trip from Earth to Mars. During the return trip, the ship must orbit the sun once, traversing an angular distance greater than 540°. Roughly six months is consumed on the outbound leg, and two and a half years on the return voyage. In January and the first part of February of 1965, the outbound trip requires a little more than a year and an angular distance of some 250°. For the return trip, the ship must again orbit the sun and arrive back at Earth after approximately two years and an angular travel of less than 540°. Late in February and March the return angular distance traveled is greater than 540°, while the outbound-voyage characteristics remain essentially unchanged. It is interesting to note that the total time of 3.2 years required for the trip does not vary by more than two months for any solution in the class.

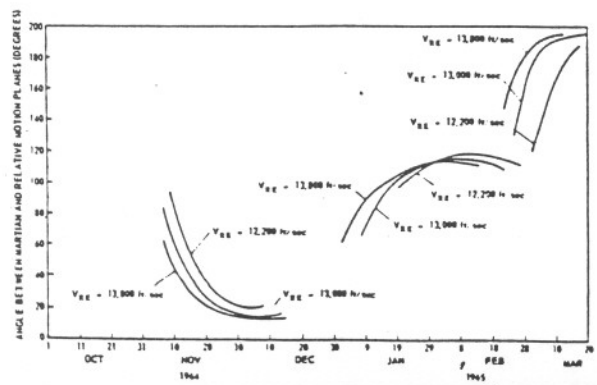

FIG. 3-13. Angle between Martian and relative motion planes vs. departure date for various values of departure velocity.

Concerning the manner of approaching Mars, the 1964 solutions require the spaceship to cross the orbit of the planet heading away from the sun. The relative motion is such that the dark side of the planet is presented to the ship during the greater portion of the period of contact. On the other hand, in 1965 the spaceship intersects the Martian orbit heading toward the Sun and the bright side of the planet dominates the field of view. In Fig. 3-13, a plot is shown of the angle between the normals of the Martian orbital plane and the plane in which the relative motion takes place. We see, for example, that in the first month and a half of 1965 the spaceship moves in a plane that is roughly perpendicular to the Martian orbital plane.

In order to gain a clearer understanding of the characteristics of these round-trip reconnaissance trajectories, a typical one has been mapped out in detail. The diagrams of Fig. 3-14 show various stages of the outbound and return trip of a spaceship departing on January 25, 1965, with a velocity relative to the Earth of 13,800 ft. per sec. The orbits of the spaceship and of Mars are shown as solid lines when above the plane of the Earth's orbit and as broken lines when they are below.

Contact with Mars would be made on April 4, 1966, when the vehicle would pass within 4,880 miles of the planet's surface. The orientation of the plane of relative motion of the spaceship with respect to the Martian orbital plane is shown in Fig. 3-14c. In this illustration, Mars is moving from right to left, the direction to the sun is indicated by the large arrow pointing toward the lower right, and the point of closest approach is shown by the small arrow. The primary effect of the Martian gravitational field is approximately to double the component of the spaceship velocity normal to the planet's orbital plane. The result, as can be seen from the diagrams, is a rotation of the line of nodes of the spaceship orbit by some 60°. Furthermore, the inclination to the ecliptic of the orbital plane changes from 0.805° for the outbound path to 2.324° for the return path, and the period is reduced from 1.53 years to 1.49 years. Finally, the vehicle would return to the Earth on March 24, 1968, after a voyage lasting 3 years and 58 days.

References

[1] Whittaker, E. T., *A Treatise on the Analytical Dynamics of Particles and Rigid Bodies*, Cambridge University Press, Cambridge, England, 1937.

[2] Wintner, A., *Analytical Foundation of Celestial Mechanics*, Princeton University Press, Princeton, N.J., 1941.

[3] Laning, J. H., Jr., Frey, E. J., and Trageser, M. B., *Preliminary Considerations on the Instrumentation of a Photographi Reconnaissance of Mars*, Report R-174, Instrumentation Laboratory, M.I.T., Cambridge, Mass., April, 1958.

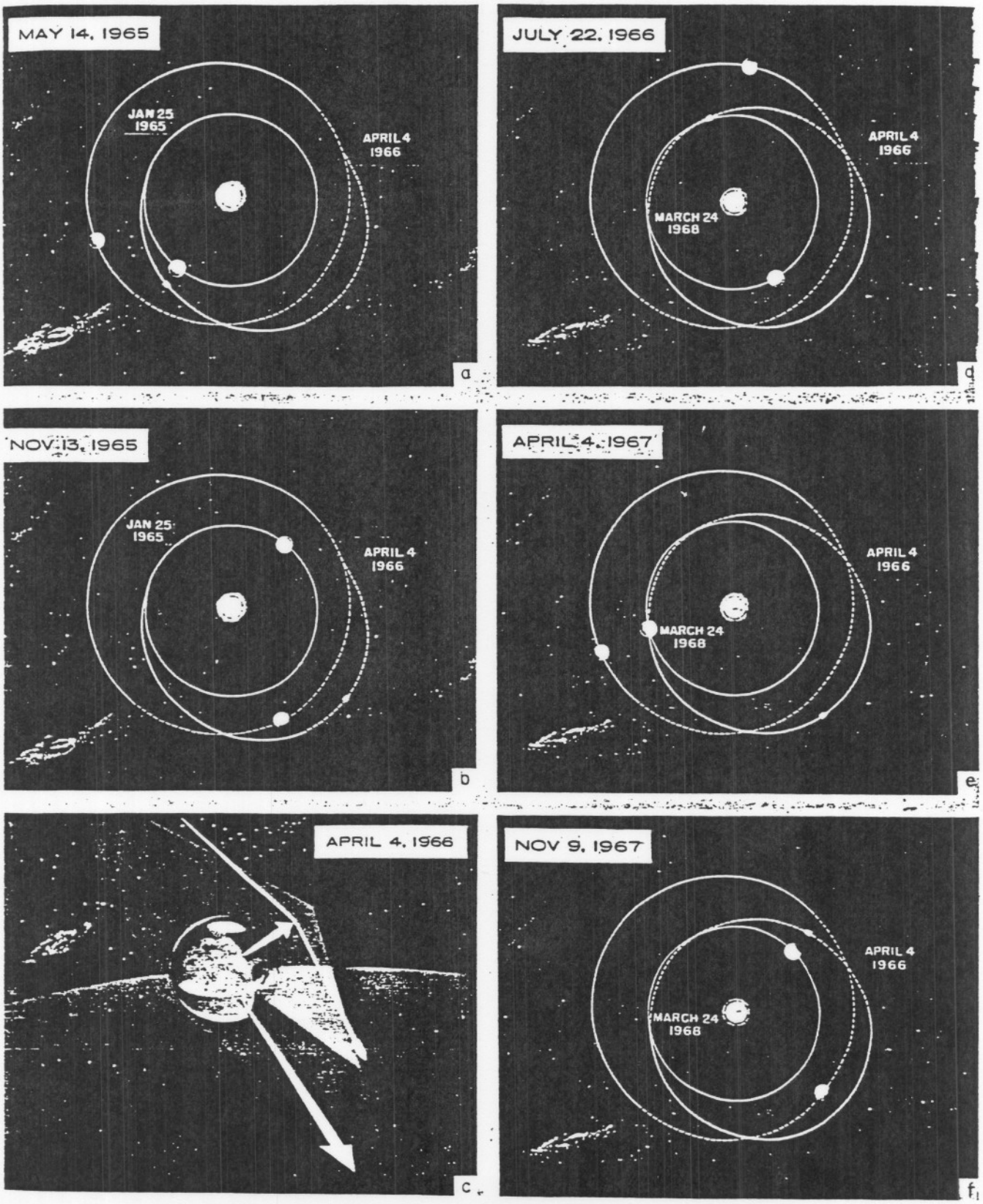

FIG. 3-14. Sample round-trip reconnaissance trajectory to the planet Mars.